PYROLYSIS BEHAVIOR OF COAL AND PETROLEUM COKE AT HIGH TEMPERATURE AND HIGH PRESSURE

by

David Ray Wagner

A thesis submitted to the faculty of
The University of Utah
in partial fulfillment of the requirements for the degree of

Master of Science

Department of Chemical Engineering

The University of Utah

May 2011

The University of Utah Graduate School

STATEMENT OF THESIS APPROVAL

The thesis of **David Ray Wagner**

has been approved by the following supervisory committee members:

Kevin J. Whitty	, Chair	**9/24/2010** Date Approved
Milind Deo	, Member	**9/25/2010** Date Approved
Jost O. L. Wendt	, Member	**9/24/2010** Date Approved

and by **Milind Deo** , Chair of

the Department of **Chemical Engineering**

and by Charles A. Wight, Dean of The Graduate School.

ABSTRACT

While pyrolysis of coal is a well-studied thermal process, little is known about pressurized pyrolysis of coal and petroleum coke. This study aims to interpret the major differences of pyrolysis via high temperature and high pressure studies with a bituminous coal, a lignite coal, and a petroleum coke. The findings of these studies will be able to expand on the narrow quantity of petroleum coke pyrolysis and offer methods of devolatilization via bench-scale laminar entrained-flow and pressurized wire-mesh heaters. In addition, the findings for the two coal ranks will add to the breadth of knowledge already published, and lend credibility to conclusions made concerning petroleum coke.

The first method explored in characterizing coal and petroleum coke pyrolysis was tests conducted at high temperature (1000 ℃ to 1400 ℃) and atmospheric pressure (13 psia). Varied oxygen content was used to switch from pyrolysis to gasification conditions and chosen based on a statistical Design of Experiments approach. Previous studies indicate that as temperature or heating rate increase, so do volatiles yield and particle swelling ratio.

The second set of experiments performed was at high temperatures as well (1000 ℃ to 1200 ℃, but the pressure was greatly increased (13 to 915 psia). This is because many industrial gasifiers are operated at higher pressures to achieve greater efficiency. The data generated will be used to predict gasifier behavior in The University of Utah's

entrained-flow gasifier and hopefully aid in commercial applications like the large dual entrained-flow gasifiers housed by Eastman Chemical Company in Kingsport, Tennessee.

TABLE OF CONTENTS

LIST OF TABLES

CHAPTER 1

INTRODUCTION

The motivation for this work began as a collaborative research project between The University of Utah and Eastman Chemical Company and was comprised of six major tasks to better understand pyrolysis and gasification processes on fundamental, yet practical levels. With this knowledge of basic concepts, correlations and connections can be made to include more dynamic and complicated instances of these two major processes. While the original Scope of Work of this collaboration included six tasks, the first four will be emphasized here because of available time and contractual obligations of the joint project. The original statements of work for these initial four tasks are outlined below.

Task 1 - Existing literature on pyrolysis and gasification behavior of coal and petcoke will be surveyed and summarized. Particular focus will be given to identifying articles that compare coal and petcoke and coal/petcoke blends. Eastman will provide access to literature reviews on pyrolysis of coal due to the extensive nature of this information. Eastman and the University of Utah will endeavor to jointly publish literature review findings. The goal will be to minimize the time at this stage and move quickly to experimental work.

Task 2 - The fuels will be sent to an external laboratory for proximate and ultimate analysis, plus measurement of heating value and ash composition. In addition,

bulk density, skeletal density, and internal surface area (BET) of the dry fuels will be measured at the University of Utah.

Task 3 - Under this task, pyrolysis and char conversion will be studied in The University of Utah's lab-scale, non-pressurized laminar entrained-flow reactor. For each fuel, char will be formed by pyrolysis in nitrogen at three different temperatures: 1100, 1250 and 1400°C (2012, 2282 and 2552°F). Char yields, volatiles yields and concentrations of major gas species (e.g., CO, CO_2, H_2, CH_4, H_2S) released during pyrolysis will be measured.

Task 4 - The University of Utah's high pressure wire mesh heater is useful for measuring pyrolysis characteristics under controlled heating rates and elevated pressures. A series of chars will be formed from each fuel under at a given heating rate (1000 °C/s, 1800 °F/s) and to at least two final temperatures (1000 and 1200°C, 1832 and 2192°F). Three different pressures will be studied: 0, 300 and 900 psig. Char yields will be measured, and we will also attempt to collect and analyze the gas produced.

The fuels that were decided upon were an Appalachian region bituminous coal, a petroleum coke from the United States, and a Texas lignite.

CHAPTER 2

LITERATURE REVIEW

Since a myriad of sources exist for pyrolysis and gasification processes, the consensus of Eastman Chemical Company and the University of Utah was to focus on the tasks in reference to the Scope of Work. In addition to the specified tasks, it was proposed and concluded that the two organizations would make concerted efforts to write articles for submission to peer-reviewed journals.

It is also important to note that the search criteria was extended to include 'lignite' references as will be discussed in detail in later sections. This section of the chapter diagrams the approach of both Eastman Chemical Company and the University of Utah and the resulting structure of the literature search to achieve the best and most efficient coverage of available information.

2.1 Methodology

Here, the methodology of the search criteria is laid out for both Eastman Chemical and the University of Utah. Different article databases were used for the conduction of searches: SciFinder, Academic Search Premier, and HCAPLUS.

Eastman Chemical had already begun peer-reviewed journal article searches with respect to the Scope of Work during the fall of 2008. The searches conducted were (1) 'gasification and pyrolysis and coal and petcoke' and (2) 'gasification or pyrolysis and

coal and petcoke.' While only 15 article references were identified for the 'gasification and pyrolysis' search, 341 results were found for the 'gasification or pyrolysis,' but were a combination of patents and articles. A large portion of these 356 references was filtered and perused by Dr. Paul Fanning of Eastman Chemical before being given to the University of Utah and combined with others.

Journal article searches at the University of Utah were conducted separately with respect to keyword criteria. The two database searches were (1) 'gasification and pyrolysis and coal or petcoke' and (2) 'gasification and pyrolysis and lignite.' The keyword 'lignite' was used because Texas lignite, an additional coal, was specified for project testing at a later date. This search modification proved useful, generating 255 references, whereas the 'coal or petcoke' search identified 65 references. To optimize the amount of time and effort on the literature review, a structured approach was agreed upon by Eastman and the University of Utah. This approach is found in Table 1.

As seen in Table 1, 676 journal articles and patents were found and narrowed down to 20 articles; these are the rows specified by 'Search References Identified' to 'Best 20 Papers.' Moving down the table, articles are filtered out based on their relevance to the Scope of Work. After running the four main searches, 676 articles and patents were narrowed to 88 articles based on titles and any available abstracts of those articles. Some sources were double-counted because of the volume of references, but were accounted for at a later date. Those 88 papers were reduced to 79 based on whether or not a copy could be obtained by either Eastman or the University; nine articles could not be obtained. From the 79 papers that were acquired, the 25 most pertinent to the Scope of Work were preserved based on the abstracts and the others were placed

Table 1: Structured approach of journal article-based literature review

	Eastman		U of U		Total
	Gasification AND Pyrolysis	Gasification OR Pyrolysis	Coal OR Petcoke	Lignite	
Search References Identified	15	341	65	255	676
Abstracts of Articles Reviewed	6	15	22	45	88
Actual Papers Obtained from Abstracts Reviewed	6	15	22	36	79
Abstract Narrowing	1	5	9	10	25
Best 20 Papers	1	4	6	9	20
Best 10 Papers of the Best 20	1	0	5	4	10
Citation references from Best 10 (Top 1 per Paper)					10
Actual Citation Papers Obtained to Date					10
Total Papers Obtained to Date (U of U)					89
Total Papers Read Completely					30
Key Papers Constituting Phase 1 Literature Review					30

temporarily to the side. After reading the 25 resulting papers, the best 20 were retained and then the best 10 of those were selected. After reading the best 10 papers again, one reference was chosen from each and obtained for study. This method brought the number of peer-reviewed articles obtained to a final quantity of 89 papers. The 20 best papers from the original 79, in addition to the 10 key references from the 10 best papers, allowed a focus to be placed on 30 key articles; this was the first phase in the literature search.

The first phase of the literature review consisted only of English articles; in the interest of time, foreign language papers were temporarily ignored. These 30 papers had publication dates between 1975 and 2008 from countries across the world, mainly the United States, Japan, and Australia. The foreign language articles were perused with respect to the abstracts, all of which were available. Twenty articles were decided upon, which were then narrowed down based on two factors: (1) how much it would cost to have the article translated and (2) if the article was attainable. Some prices far exceeded what the paper would contribute to the project's body of knowledge and other papers would simply repeat some information already diagramed in other articles. This process produced three articles that were obtained and translated, two were in Chinese and one was in German. These three papers were translated and added to the 88 already obtained in English, bringing the total number to 91 peer-reviewed journal articles.

All references that were not journal articles were deemed hardcopy sources because the bulk of them were not available from online (Internet) sources, but were checked out from the Marriott Library or borrowed from the Chemical Engineering Department of the University of Utah. These references consisted of two major encyclopedias, The Kirk-Othmer Encyclopedia of Chemical Technology and Ullmann's

Encyclopedia of Industrial Chemistry, along with 12 books including the Chemistry of Coal Utilization: Second Supplementary Volume by H. H. Lowry.

Pertinent sections of the encyclopedias and books included the same keywords as the journal article searches like gasification, pyrolysis, coal, and petcoke in addition to chapters concerning previous work on gasification systems and processes. The main process examined was the Texaco gasifier system because the Kingsport, Tennessee facility of Eastman Chemical was the first commercial operation of such a system.

2.2 Fuel Characterization

This section follows the outline found in the Scope of Work with the following task description.

The fuels will be sent to an external laboratory for proximate and ultimate analysis, plus measurement of heating value and ash composition. In addition, bulk density, skeletal density, and internal surface area (BET) of the dry fuels will be measured at the University of Utah.

2.2.1 Description of Analyses

2.2.1.1 Proximate Analysis

A proximate analysis is the determination of moisture, ash, fixed carbon, and volatile matter content; the percentages of these four groups add to 100 percent. During the analysis, water is driven off first and then volatile matter, including hydrogen, carbon monoxide, and combustible hydrocarbons as well as tar vapors and inert gases like

carbon dioxide [1]. The fixed carbon is the carbon skeleton left after devolatilization and the ash is the sum of all mineral matter and impurities.

2.2.1.2 Ultimate Analysis

As with proximate analyses, there are many different methods to conduct an ultimate analysis, such as ASTM or ISO standards, but all quantify the percentages of carbon, hydrogen, nitrogen, oxygen, sulfur, and ash. This elemental composition is vital when conducting material balances and deciding which fuel to use for gasification, for if too much sulfur is present, then it must be cleaned or scrubbed out downstream of the process to meet environmental standards. In addition, since proximate, ultimate, and calorific analyses are performed with various methods, it is vital to state on which basis the values are being reported. Three reporting bases exist: (1) as received, where no pre-treatment of the fuel is performed, (2) dry or moisture-free, where all moisture is driven off the fuel sample before analysis or the values are adjusted to neglect moisture, and (3) dry, ash-free, where the reported values are adjusted to neglect ash and moisture. Sulfur forms and ash are discussed in detail in later sections [1].

2.2.1.3 Calorific Analysis

This analysis is performed to determine the amount of energy capable of being extracted from a fuel on a unit mass basis. Typical units are either kJ/kg or BTU/lb.

2.2.1.4 BET Surface Area Method

The BET surface area method is named after Brunauer, Emmett, and Teller (BET) and is conducted with liquid nitrogen at -196℃. The method determines the amount of surface area on a unit mass basis through adsorption of the nitrogen by the fuel.

2.2.1.5 Sulfur Forms Determination

Three main forms of sulfur exist that become important in pyrolysis and gasification processes. There are organic, pyritic, and sulfate forms of sulfur, all of which constitute the percentage of sulfur in an ultimate analysis. Since certain forms of sulfur make hydrogen sulfide and other toxic gases more readily than other forms, it is important to know the percentages of each form in the combusting or gasifying of fuel.

2.2.1.6 Ash Analysis

Within a single ash analysis, many different mineral forms and impurities exist. Mainly oxides are produced including aluminum, calcium, iron, magnesium, and titanium, but silicates and sulfates are produced as well. The ash content becomes important when measuring slag viscosity and deciding on the most efficient method of disposing of the ash in gasification processes.

2.2.1.7 Density Methods

Two types of densities are important in potential feedstocks, bulk and skeletal. Bulk density can vary depending on the void fraction of the sample and how well the fuel is packed together, where void fraction is the dimensionless value of all spaces or ‘voids’ between particles, also taking into account larger pores. The skeletal density takes into

account the fact that particles are not spherical and quantifies the mass of the carbon skeleton that the particle constructs. This density is much more difficult to measure because few substances are capable of penetrating all the pores of a fuel particle, whereas bulk density is simply the mass of a container, fuel plus voided volumes, divided by the volume of the container. ASTM methods exist to calculate the skeletal density by helium or hydrogen pycnometry, where a container of specified volume is filled with a known mass of fuel and the void spaces are filled with the sample gas, hydrogen or helium, and weighed. The mass of gas introduced to the known volume is then calculated, leaving the mass of the fuel particle divided by the volume of which the particle occupies, giving skeletal density.

2.2.2 Surveyed Fuels

The primary focus of the surveyed literature was fuels within the United States. U.S. fuels were primarily sought out because Eastman Chemical uses these kinds of fuels for gasification. Many Appalachian coals were found in the literature, mainly from the Pittsburgh number 8 seam, Illinois number 6, and Kentucky. Table 2 contains the analyses and rank of available data concerning the fuels found in the top 30 articles constituting phase one of the literature search. While fuels from the United States were the focus of the literature review, it is also important to understand how much coal and petcoke can vary from country to country. The fuels found in the top 30 articles are presented in Table 3 according to geography. While Table 2 and Table 3 are specific with respect to geography, Table 4 shows the frequency of all 81 named fuels in the top 30 articles with respect to available analyses and rank.

Table 2: Fuel attributes of U.S. coals found in top 30 articles of literature review

Fuel Attribute	Frequency
Petcoke	1
Lignite	7
Bituminous	17
Sub-bituminous	5
Proximate analyses	26
Ultimate Analyses	22
Bulk Density	0
Surface Area	6
Ash Analysis	0
Petrographic Analyses	2

Table 3: Geography of top 30 articles reviewed, containing 81 fuels

Geographic Region	Frequency
United States	30
Australia	10
Asia	10
Europe	15
Other	7
Unspecified	9

Table 4: Frequency of analyses and rank of top 30 articles' fuel sources, contains 81 fuels

Overall	
Named Fuels	81
Geographies	24
Proximate Analyses	65
Ultimate Analyses	63
HV Analyses (BTU content)	16
Bulk Density	6
Surface Area	12
Ash Analysis	7
Petrographic Analyses	19
Fuel Type	
Petcoke	9
Lignite	17
Bituminous	38
Sub-bituminous	10
Anthracite	3
Unspecified	4

2.3 High Temperature, Atmospheric Pressure Entrained-Flow Reactor Studies

This task primarily focuses on the initial reactions that lead to carbon conversion. Since pyrolysis is the first major process that fuel undergoes to create volatile gases, tars, oils, and char, it is vital to understand the key mechanisms of the process. Evolution of volatiles and resulting char morphology are focused on in this section with respect to variable temperature, pressure, heating rate, and particle diameter. Below is the task description for the high temperature, atmospheric pressure study as per the Scope of Work.

Under this task, pyrolysis and char conversion will be studied in The University of Utah's lab-scale, non-pressurized laminar entrained-flow reactor. For each fuel, char will be formed by pyrolysis in nitrogen at three different temperatures: 1100, 1250 and 1400°C (2012, 2282 and 2552°F). Char yields, volatiles yields and concentrations of major gas species (e.g., CO, CO_2, H_2, CH_4, H_2S) released during pyrolysis will be measured.

2.3.1 Volatiles Evolution

2.3.1.1 Temperature Dependence

Because so many different species evolve during coal and petcoke pyrolysis, defining the different components becomes a necessity. The lighter species consist of water vapor, carbon monoxide, carbon dioxide, methane, hydrogen, and hydrogen sulfide [2]. Heavier species are larger hydrocarbons (e.g. ethane, propane, and propylene), and aromatic compounds (e.g. benzene, toluene, and xylene). All surveyed literature agrees that with an increase in temperature, more volatiles are emitted from the coal [3], [4], [5].

In Coal Combustion and Conversion Technology [6], it was found that lower temperatures caused the conversion process to be more kinetic-dependent and influenced by the concentrations of species. On the other hand, higher temperatures caused conversion to be more dependent on diffusion rates, likely because of partial pressures and dominant mass transfer effects. The two major sections of the Kirk-Othmer Encyclopedia qualitatively describe many interactions with respect to temperature and incorporate pressure and individual species production. As seen in the previous section, fuel characteristics have a great deal of influence on how a system operates and accounts

for differences in fuel types. Tar yield is heavily dependent upon the rank of coal being pyrolyzed where higher temperatures reduce tar production, increasing the cracking of tars to light gases. These higher temperatures will favor the endothermic water-gas reactions, primarily the well-known water-gas shift reaction where carbon monoxide and hydrogen are produced from water and carbon dioxide. High temperatures also explain why the methanation reaction can be a hindrance at times; in this reaction, the products of the water-gas shift reaction further react to form methane and water. The Kirk-Othmer Encyclopedia also describes that when temperature is increased, there is a tendency for a reduction in moles in chemical reactions; methanation is a perfect example where four moles are reduced to two with an excess of heat.

The occurrence of the secondary reactions described above (e.g. methanation and hydro-gasification) was found in the literature mainly concerning residence time in which secondary reactions were minimized by shortening the time fuel was allowed to react. Initial reactions generate small molecules or slightly transform larger ones, but if the species are allowed to have a longer residence time, they will interact with others and produce larger compounds. Concentrations of water, carbon monoxide and dioxide, hydrogen, and methane are plotted in Figure 1 with variable temperature to show thermal dependence.

2.3.1.2 Pressure Dependence

Pressure effects are not as common as those of temperature, but more studies are being performed in an attempt to create valid models to predict gasification processes.

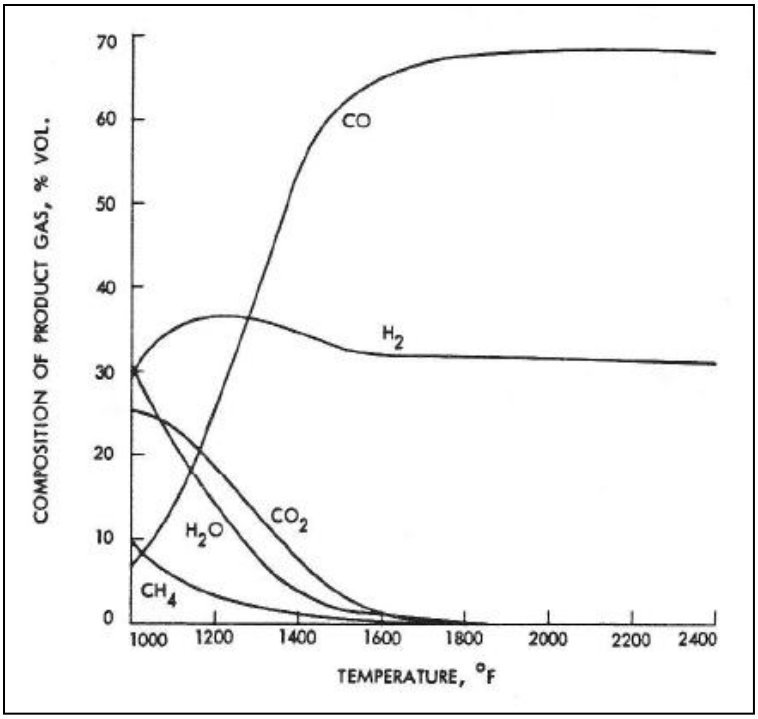

Figure 1: Equilibrium gas composition versus temperature [7]

Similar to the temperature effects on tar evolution, as pressure increases, the tar yield decreases. Concerning volatiles, however, overall yields decrease as pressure increases. The Kirk-Othmer Encyclopedia specifically considers hydrogen and carbon monoxide, writing that the concentrations increase with decreased oxygen feed, high temperature, and lower pressure. This could translate to the methanation reaction because the higher the pressure, the more methane is produced, consuming the available hydrogen in the system. One of the major causes for such behavior in a pressurized gasification system could be attributed to le Chatlier's Principle where the partial pressures of the gases drive the chemical reactions forward or in reverse, but it is important to remember that this principle indicates a system at equilibrium.

2.3.1.3 Heating Rate Dependence

Most high temperature data were gathered with atmospheric pressure resulting in good sources of qualitative and quantitative information for Task 3 testing. Since this task is at atmospheric pressure with high temperatures, heating rates could become very important in the evolution of volatiles. If the heating rate is low enough, pyrolysis will begin between 250 and 325 ℃ and becomes instantaneous at about 700 ℃ [7],[8]. In addition, since the heating rates for such experiments could be based on the feed rates of air or oxygen and the feedstock, it is important to understand how the oxygen concentration influences pyrolysis. As the oxygen to fuel ratio is increased, carbon conversion is also increased; this is evident of gasification processes becoming combustion processes [9]. Coal rank also has a significant impact on the gasification rate of a feedstock. In Coal Science and Technology [7], anthracite and coke were written as consuming approximately three times as much oxygen as lignite in pyrolysis and gasification processes.

2.3.2 Char Morphology

2.3.2.1 Particle Diameter

As expected, all literature shows that particle diameter changes as pyrolysis time is increased. The most common model that is used in analyzing data is the shrinking-core model where diameter decreases as reaction time is extended [9]. This theory states that a coal particle becomes smaller as the water and volatiles are evolved, ultimately leaving a carbon skeleton of char. This is the common and almost decided upon model that is used to approximate coal pyrolysis with respect to particle diameter and pyrolysis time. On

the other hand, it has been determined that particle swelling occurs, mainly influenced by gasification pressure. Dr. Thomas Fletcher of Brigham Young University showed that significantly lower swelling ratios exist at elevated pressures, where swelling ratio is defined as the final particle radius divided by the initial radius [10]. He also found and validated that there is a substantial decrease in particle swelling as heating rates are increased from a magnitude of 10^4 to 10^5.

Since carbon conversion is the basis of gasification, it is also vital to understand what influences that process and what can be improved. It has been shown that as feed particles become smaller, carbon conversion increases. This is most likely attributed to the fact that higher mass fluxes are possible with smaller particles and volatiles and tars have less distance to travel before being liberated from the coal or petcoke particle.

2.3.2.2 Temperature Effects

While most temperature effects have already been discussed, there are specific details that deserve their own section. Kinetic parameters are very influential in the evolution of volatiles and tars, and have been shown to vary with respect to the thermodynamics of a gasifying system. In a United States Department of Energy report, it was shown that the oxygen and char reaction was zero order for temperatures below 925 ℃ and first order from temperatures ranging 925 to 1925 ℃ [9]. This is also evident of the driving-force dependency with respect to temperature where systems are chemically driven at lower temperatures and are thermally driven at higher values.

2.4 Investigation of Pyrolysis Behavior in a High Pressure Wire Mesh Heater

In order to understand pyrolysis and gasification behavior of fuels, a method of rapid heating was devised to simulate the environment of large-scale gasification plants.

2.4.1 Pressure Effects

Several studies have investigated the influence of pressure on devolatilization behavior of coals[1-8]. Experiments at very low pressure (<1 Torr) were conducted in a wire-mesh heater in which alternating current was used to heat the system ranging from 0.1 to 5000 ℃/s [11]. Gibbins demonstrated that heating rate effects were independent of geometry and that volatile and tar yields increased about six percent d.a.f. with heating rate in an inert atmosphere (helium) under this high vacuum. It was also shown that if the pressure or particle size was increased under rapid heating conditions, only minor pressure effects were present for lignite. With lignite, however, significant increases in hydrocarbon and char yields were evident with a decrease in tar yields, but only if the final temperature was above 800 ℃ [12]. Sathe et al. focused on super-elevated pressures with Australian lignite and found a sharp decline in tar yield at lower temperatures and pressures up to 20 bar[13]. Figure 2 displays three plots of tar evolution versus pressure under heating rates of 1000 ℃/s with 10 second holding times, reaching final temperatures of 900, 700, and 600 ℃, respectively. A sharp decline in yield is seen at lower temperatures and as pressures exceed 20 bar (275 psig), the tar yield becomes more level and the slope of the curve decreases.

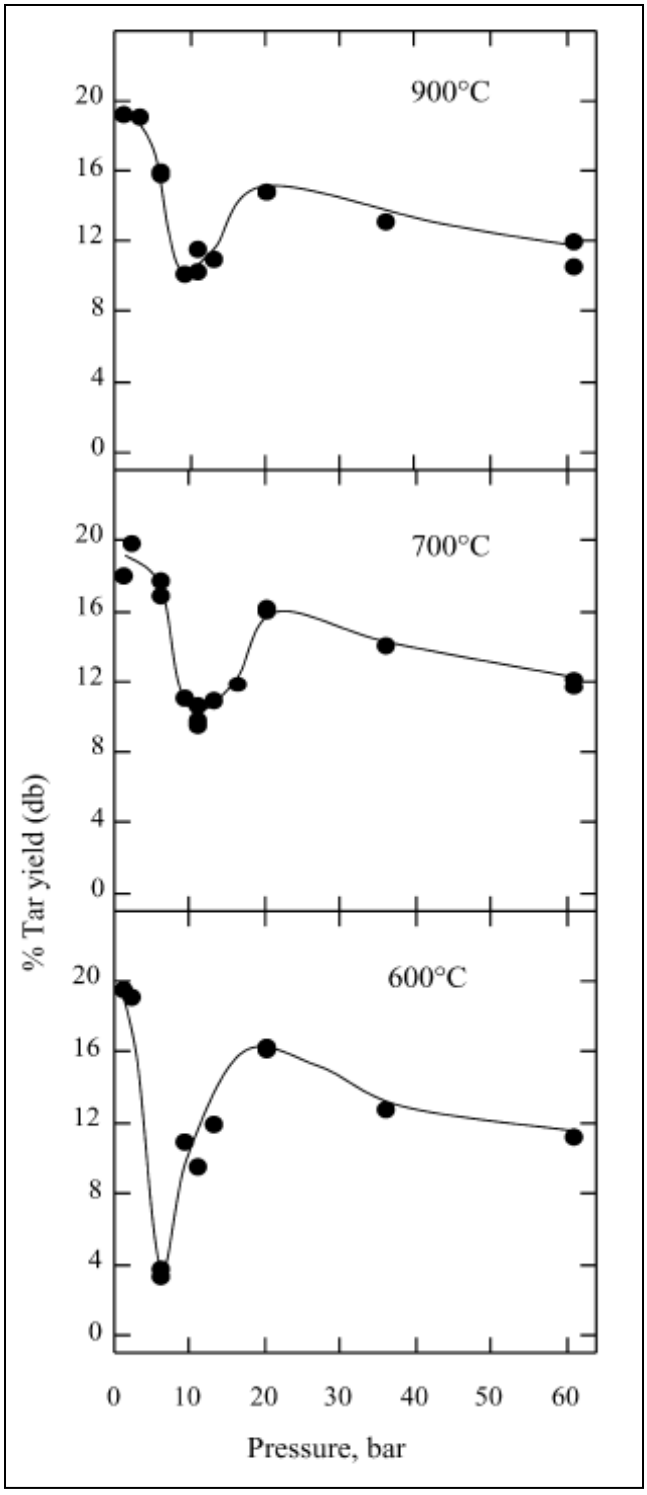

Figure 2: Tar yield versus increasing pressure of lignite with heating rate of 1000 ℃/s with a 10 s holding time at 900, 700, and 600 ℃ [13].

A separate study was conducted with Pittsburgh seam coal (bituminous), yielding different results. The discrepancies may be attributable to the different coal ranks or may be an inconsistency in the data and methods. Figure 3 shows the yields for methane, other hydrocarbon gases, tars and liquids, and total volatiles with varying particle diameter versus pressure. To achieve an inert atmosphere for testing, helium was used along with two to ten second holding times for the samples under 1000 °C/s heating rates reaching a constant final temperature of 1000 °C at pressures up to 85 bar [12].

The evolved gas species themselves may influence the char conversion process and indirectly increase the volatiles yield [4]. As the partial pressure of hydrogen is increased, volatiles yield is increased, but if the system pressure is increased, then the volatiles yield is decreased. The occurrence of such an effect also increases volatiles yield by directly decreasing the amount of char produced, causing the reaction to be interrupted by the relatively high partial pressure of hydrogen [4].

2.4.2 Particle Effects

It was found that higher heating rates increased overall volatiles yield [8]. This effect could be attributed to the gas-gas and gas-solid reactions occurring simultaneously with higher heating rates. With lower heating rates, however, volatile yields were shown to decrease as a result of repolymerization of coal particles [3]. Also, with rapid heating rates (400-100,000 °C/s), volatiles yields were 20 to 40% more than with slow heating rates [3], [7].

The most prominent diffusive effect from the literature was that as particle size is decreased, higher volatile yields are achieved [4]. This would stem from higher fluxes

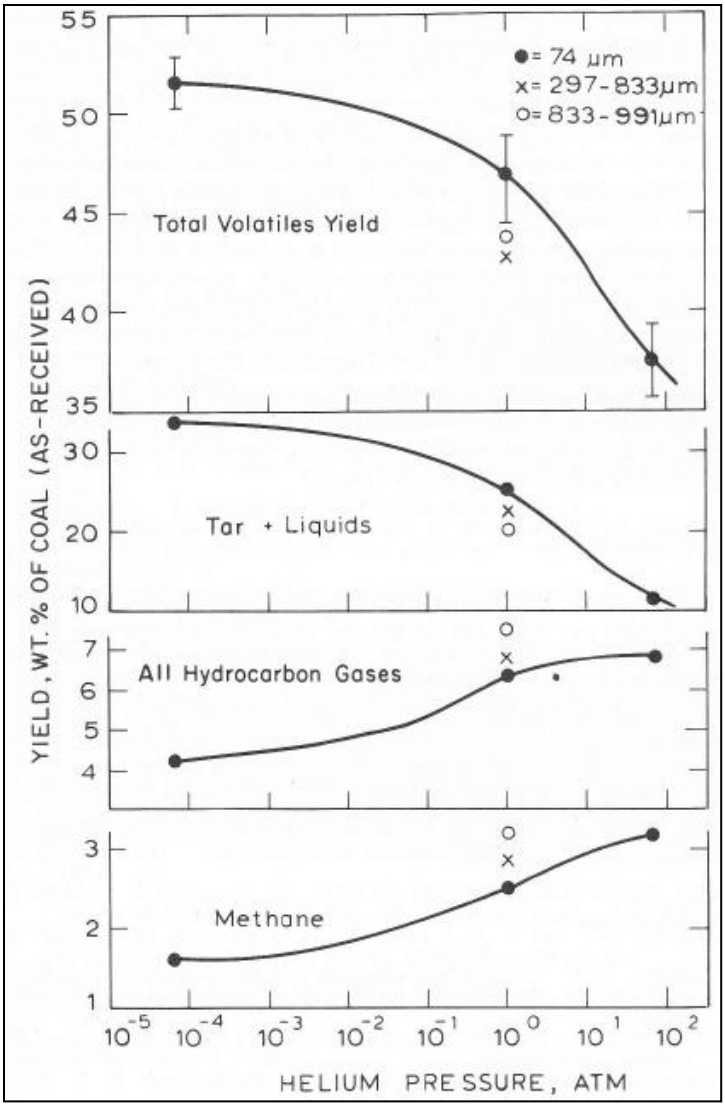

Figure 3: Total volatiles yield (%) with increasing inert atmosphere of a bituminous coal with a heating rate of 1000 ℃/s and variable holding time (2-10 s) and a temperature of 1000 ℃[12].

across the boundary layer of the particle by lowering the surface area through which the gases travel; relatively more mass would be transported in less time, thereby increasing the volatiles flux from the particle. Parallel with heating rate effects are pressure influences on the rate of diffusion of both tars and gases from fuel particles. It was found that an increase in pressure slowed rates of diffusion, especially for aromatic ring systems captured in the tars, but an increase in the partial pressure of hydrogen had the opposite effect, converting coal to gaseous and liquid products more readily, particularly benzene, toluene, and xylene.

2.4.3 Atmospheric Effects

In previous grid-heater studies, three environments have been used: helium, argon, and hydrogen. There were no discernable differences in the atmospheres used for the various wire-mesh studies with the exception of hydrogen, which increased volatiles yield 10 and 15 percent with respective heating rates of 5 and 1000 ℃/s under a pressure of 70 bars. Also, since both helium and argon are inert gases, there was no distinct difference in the level of volatiles produced, unlike any case with hydrogen [14]. The instance of hydrogen being used is in agreement with other non-wire-mesh studies where an increase in partial pressure of hydrogen increases volatiles yield. Hydrogen is a reactive species that can (1) consume carbon via the following reaction:

$$C_{(s)} + 2H_{2\,(g)} \rightarrow CH_{4\,(g)}$$

and (2) crack aromatic hydrocarbons.

2.5 Assessment of Performance in a Pressurized Entrained-Flow Gasifier

Three common gasifiers are used in industrial processes more than any others, a moving-bed, fluidized-bed, or entrained-flow gasifier [15], [8]. Many advantages and disadvantages exist for any gasifier, but the entrained-flow reactor will be discussed extensively throughout this section because of the pilot-scale facility at the University of Utah. Though much literature was read and perused with respect to gasification, few sources were in direct relation to entrained-flow processes. The articles that most closely approximate the University of Utah's facility were focused on and trends concerning dry gas compositions, process measurements, and operating pressures were looked at as other sources in hopes of constructing a table of cause and effect related aspects under high temperature and high pressure gasification processes.

All surveyed literature agreed that entrained-flow processes require the smallest particle size for gasification processes [3], [16]. This is because larger particles require more energy to transport through the reactor and the gasifier will lose efficiency. In addition to the particle size, caking properties must be taken into consideration in order to predict gasifier behavior. Decaking of feedstocks has been performed with additives such as dry sand, sodium carbonate, and sodium hydroxide with Kentucky No. 9 and No. 11 seams [17]. Sodium hydroxide proved to be the best decaking treatment for these bituminous coals, which swell and agglomerate at temperatures in the range of 300-350 ℃ [3]. This agglomeration can create a larger dilemma when considering the relatively short residence time of entrained-flow processes, being on the order of one to five seconds [3], in which rapid heating rates are also exemplified stemming from such high temperatures [8].

These high temperatures mainly exist from more oxygen being present in entrained-flow processes, resulting in flame temperatures that can exceed 2000 ℃ (Ullmann's). Excessively high temperatures then cause much higher heat losses than other gasifiers and lead to lower efficiencies [16].

Ullmann's Encyclopedia of Industrial Chemistry lists many advantages and disadvantages to entrained-flow processes summarized below.

Advantages of entrained-flow processes:

1. Multiple designs exist for commercial use.
2. Gasification processes contain the highest capacity per unit volume.
3. There are no moving parts, thus less maintenance.
4. No particle fines are rejected due to entrainment.
5. Product gas (syngas) is free of tars and heavy oils.
6. Any rank of coal may be used for gasification processes.
7. The process produces inert slag with a low carbon content.

Disadvantages include:

1. Heat recovery is vital, especially in the presence of molten slag.
2. Pulverization of gasifier feedstock is necessary.
3. Drying of feedstock is required (to below ~5%) unless slurry feed system is used.
4. High temperatures result in more heat losses and higher costs in construction materials.

One entrained-flow study characterized a pressurized reactor in terms of operating wall temperature, feed rate, and equivalence ratio (the article referred to this as stoichiometry, where a 100% stoichiometric mixture was a one-to-one ratio of oxygen to

carbon) [5]. The study was performed at pressures of 290 psi and a nitrogen atmosphere with 2.5% oxygen. Resulting equivalence ratios were altered by changing the coal feed rates from one to five kg/hr, adjusting the stoichiometry from 50 to 200%; reactor wall temperatures were held anywhere between 1100 and 1500 ℃. The study showed that an optimum stoichiometry exists between 90 and 100% for coal gasification with respect to coal conversion and product gas quality [5]. Another study showed that as pressure is increased (with a maximum of 300 psi), there is a small but consistent reduction in char reactivity and that tar yield decreases by 25% when increasing pressure from 44 to 190 psi [18]. In an effort to make the information discussed throughout this paper more understandable, major trends with respect to process variables and performance are tabulated in Table 5. Since not all effects are caused by an increase in a specific variable, Table 6 shows the effects of decreasing process variables and parameters.

2.6 Summary of Literature Review Findings

When reading the compiled body of knowledge comprising this literature review, few aspects stand out as unexpected or out of the ordinary. As expected, however, many temperature trends and results followed previous literature and a general knowledge of gasification. Prior to completing this review, less information was known concerning residence time and heating rate effects, but the results were followed carefully and are now understood with respect to temperature. Diffusion effects also follow as expected by extending the results to mass transfer and kinetic theory to gain an elevated comprehension of the findings. On the other hand, pressure effects are less understood than other effects. This is attributable to less available pressure data whose results seem

Table 5: Overall trends with increasing process variables or parameters

Increase In:	Has this directional effect:	Constant Parameters and additional notes
Temperature	Increase in volatile yields	2-4% over 1000 °C increase
	Decrease tar production	
	Increase in methane production	from methanation reactions
	Decrease in mole production by means of chemical reactions	
	Increase in initial char reactivity	Effects enhanced with low coal rank
	Increase in gasification rates	
	Increase in oxygen/char reaction orders	
	Increase in carbon conversion	At atmospheric pressure
	Decrease in gasification rates (T>1150 °C)	At atmospheric pressure
	Increase in gasification rates (T<1150 °C)	At atmospheric pressure
	Decrease in oxidation reactivities of char	At atmospheric pressure
Pressure	Increase in H/C and O/C ratios	From 1 to 6 atmospheres
	Decrease in swelling ratio	
	Decrease of lignite and bituminous char reactivities	
	Leads to a ~25% decrease in tar production	In the range of 44 to 190 psi
	Overall decrease in tar production	20% to 12% over range of 870 psig
	Sharp decrease of 10% in tar yield (0 - 145 psig)	
	Sharp increase of 7% in tar yield (145 - 275 psig)	
	Slight decrease of 4 % in tar yield (275 - 870 psig)	
	Overall decrease of volatile yields	
	Decrease in diffusion effects	Gas partial pressures influence rate laws, less yield by ~15%
	Release of tars is greatly delayed (~10 seconds at 145 psig)	
	Decrease in heating rate sensitivity of tar yield	
	Decrease in aromatic ring systems (~25%)	
	Increase in char surface area, follows same trend as tar yield	

Table 5: Continued

Increase In:	Has this directional effect:	Constant Parameters and additional notes
Heating Rate	Decrease in swelling ratio	
	Increase in tar yield	~5% over 2000 °C/s range
	Increase in volatiles yield	2-4% over 2000 °C/s range
	Increase in particle size	Swelling occurs
	Decrease in char formation	
	Increase in devolatilization rates	
Pyrolysis Time	Decrease in particle diameter	
	Decrease in char production	
	Increase in volatiles yield (12-15% over 200 seconds)	
	Decrease in char reactivity	
	Decrease in initial char gasification rates	
Coal Rank	Increase in oxygen consumption for gasification	
H_2 Partial Pressure	Increase in volatile yields	
Volatile Yields	Decrease in char production	
Char Density	Increase in char reactivity	

Table 6: Overall trends with decreasing process variables or parameters

Decrease In:	Has this directional effect:	Constant Parameters and additional notes
Heating Rate	Decrease in volatile yields	Repolymerization occurs
Particle Size	Increase in volatile yields	
Coal Rank	Decrease in devolatilization temperature	Initial temperature, not necessarily final
Coal Rank	Decrease in swelling	
Char Production	Decrease in char reactivity	

more subjective than do others. For example, one journal article may characterize the pressure effects as minimal when another states that the effects are anywhere from slight to moderate. These differences may stem from different data acquisition systems, human error during experimentation, or the authors' interpretation of the data. The high pressure studies, in particular, hope to put the available pressure data in context by measuring yields at 0, 300, and 900 psig. With this broad range, the literature data summarized in this report will hopefully lend validation to the project results and allow for a more complete database with respect to pressure measurement and data acquisition.

After reading the literature thus far, it is clear that there is no one large portion of missing data that could be claimed to constitute a large gap in the body of knowledge. Minor instances do exist, mainly with inconsistent pressure analyses as described above where the qualitative analyses are more subjective than are others, but quantitative data lend the basic level of understanding required to decipher and compile those data. Few articles and other sources were able to offer a wide range of pressures, which makes those sources that much more important. The high pressure study findings will be compared to the articles with similar pressure ranges, and correlations will be found to validate the project's Scope of Work. With respect to the available literature and the corresponding body of knowledge, it appears that the Eastman Chemical Company and the University of Utah collaboration will mainly contribute to advanced understanding of temperature and pressure effects dealing with the gasification properties of coal and petroleum coke. The elevated temperatures of the high temperature, atmospheric pressure study will allow many profiles to extend beyond about 1200 ℃. Most literature concerning devolatilization extends to this temperature, but not much reveals data beyond this point.

Specified temperatures in the Scope of Work are 1100, 1250, and 1400 ℃, allowing for volatile species evolution characteristics to be extended by about 200℃. In addition, as stated above, pressure effects and subsequent gasification processes will be understood at a higher level than before.

CHAPTER 3

EXPERIMENTAL

3.1 Entrained-Flow Pyrolysis Studies

3.1.1 Experimental Approach

This section describes the process and reasoning of moving from a one-factor-at-a-time experimental design to a more sophisticated Design of Experiments approach (DoE). Char yield determination is also discussed because of its altering experimental method and differing rationale.

The initial design was to test each parameter as described in the Scope of Work. To optimize man-hours and the quality of data produced, a statistical Design of Experiments was proposed by Dr. Paul Fanning and Dave Stevens of Eastman Chemical Company. After deliberation of available statistical paths, a Design of Experiments was agreed upon and followed as seen in Table 7.

Three unspecified oxygen ratios were proposed in the Scope of Work that were later resolved to be oxygen-to-carbon (O/C) ratios of zero, one, and two, as seen in Table 7. These values facilitate assessing the validity of gas-phase results by applying simple combustion theory. When analyzing subsequent data, this was used as a qualitative indicator, where the CO_2 percentage in particular increased if the oxygen level increased.

Table 7: Final Design of Experiments with corresponding test run numbers

		Temperature, ℃		
		1100	1250	1400
O/C Ratio	0	3	7	4
	1		1,6	8
	2	5		2

The three corresponding temperatures are also seen in Table 7, where 1400 ℃ is the only temperature that is used at all three O/C ratios, as per the Scope of Work.

Physical limitations exist within the laminar entrained-flow reactor (LEFR) that make it impossible to determine char yield without subsequent experimentation using the product char. Prior to the experiments of this project, it was known that a complete mass balance could not be performed on the LEFR because of wall effects, attracting fine particles and tars from the high temperatures. This section describes the process of additional tests and the rationale of why they needed to be performed.

Suhui Li, a doctoral student under Dr. Kevin Whitty of the University of Utah, had been performing tests with the LEFR for over one year using ash as a tracer to effectively close a mass balance. Working on the principle that ash does not react within the system, and can therefore be deemed inert, Dr. Li calculated carbon conversion of his samples. Using the same principle of ash conservation, a simple expression for char yield was established for Task 3.

$$Char\ Yield = \frac{Ash\ \%\ of\ Fuel}{Ash\ \%\ of\ Char} = \frac{\frac{mass\ ash}{mass\ fuel\ (dry)}}{\frac{mass\ ash}{mass\ char(dry)}} = \frac{mass\ char\ (dry)}{mass\ fuel\ (dry)}$$

This equation states that if the ash percent of parent fuel (on a dry basis) and the ash percent of a given char are known, then char yield is simply the ratio of the two. The percentages of ash for parent fuels and produced chars were determined using a method derived from the ASTM standard for proximate analysis [19]. The principle of ash as a tracer is seen in Figure 4.

From Figure 4, if the ash content (blue) of the parent fuel is 10%. This ash passes through the reactor and is contained in the char. The same can be said for the nonash matter lost in the muffle furnace (red), which would include mostly fixed carbon. The approximately 40% lost in the LEFR (green) would be major gas species such as H_2O, CO, CO_2, H_2, and SO_x as well as tars and other complex hydrocarbons. Therefore, char would be the 60% matter left over. The only explicit assumption of this method is that the material "lost" to the reactor is in the same proportion as in Figure 4; that is, for every 10% of ash unaccounted for, there is 90% other matter unaccounted for as well, 40% of which is termed volatiles.

3.1.2 Apparatuses and Procedures

This section presents the apparatus used for the high temperature, atmospheric pressure tests along with char yield and loss-on-ignition apparatuses followed by their respective procedures.

3.1.2.1 Laminar Entrained-Flow Reactor

The reactor in which all high-temperature, atmospheric-pressure tests were carried out was a laminar entrained-flow reactor. It was fabricated at the University of Utah with

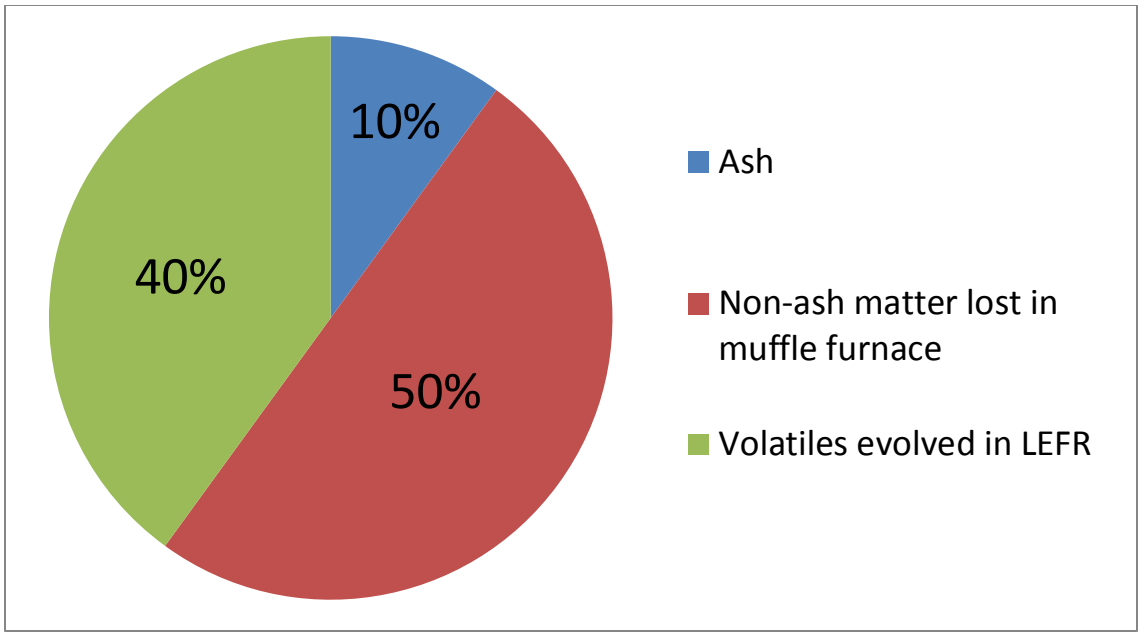

Figure 4: Ash tracer principle applied to char yield determination

an alumina tube running the length of the reactor inside of a clam-shell type furnace. The whole system consists of a high temperature furnace, a coal feeder, a sample collector (cyclone), compressed gas supply, and cooling water circulation. Two co-axial alumina tubes (89 mm O.D. × 75 mm I.D. × 1500 mm long and 57mm O.D. × 50 mm I.D. × 1000 mm long, respectively) are mounted vertically inside the furnace and sealed with specially machined flanges. The furnace itself is made by Carbolite with a single zone 610 mm in heated length with 1600 °C maximum operation temperature. The reaction gas is injected through three injection ports on the bottom flange, preheating the gas as it flows upwards through the annulus between the two co-axial tubes. When the reaction gas reaches the top of the annulus, it turns and flows down into the inner tube through an alumina honeycomb flow straightener. The flow straightener has a sufficient pressure drop to generate a uniform and laminar flow, which is essential so the entrained particles can travel along the centerline of the reactor tube, being subjected to the same reaction

conditions. Fuel particles are fed to the reactor through an injection probe using a vibrating syringe pump as a fuel feeder with nitrogen as the carrier gas. The injection probe is water-cooled to prevent the fuel particles from being heated before reaching the reaction zone. After pyrolysis or gasification reactions occur, products exit the reactor through a water–cooled collection probe and particles are collected in a cyclone. Nitrogen is injected into the collection probe through a sintered stainless steel tube to quench the product stream and reduce the deposit of char particles on the colder surface of the probe. An inline filter captures fine particles before sending a gas sample to a gas chromatograph or a vent hood.

Based on previous testing, the highest allowable temperature is 1400 ℃, which is a limitation of the alumina tube; at high temperatures (>1300 ℃) and pressures exceeding atmospheric, the tube becomes exceedingly malleable and easy to warp or break. Temperature profiles as a function of reactor length can be seen in Figure 5, characterizing the temperature controller used for the furnace. The controller is made by Carbolite, type STF 16/610, with a maximum temperature and amperage of 1600 ℃ and 50 Amps, respectively, requiring 208 V, single-phase power capable of 7 kilowatts at 50-60 Hertz. A detailed cross-section of the LEFR can be seen in Figure 6 and a schematic can be seen in Figure 7. The cross-sectional view details the flow inside the reactor including the honeycomb flow straightener and carrier and flow gases.

From Figure 6, the collection system is diagramed with a cyclone to filter out relatively small particles and collect what is termed as char. The sample pump and subsequent sampling systems are diagramed in Figure 8.

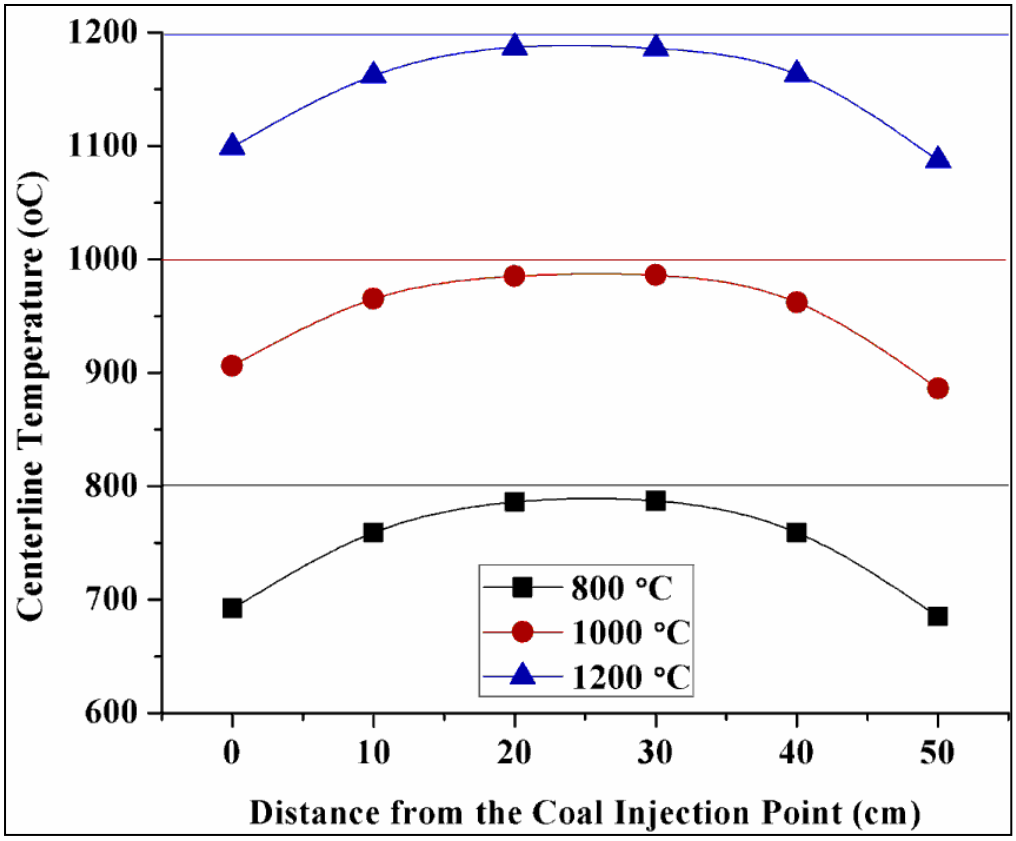

Figure 5: Longitudinal temperature profiles of the laminar entrained-flow reactor

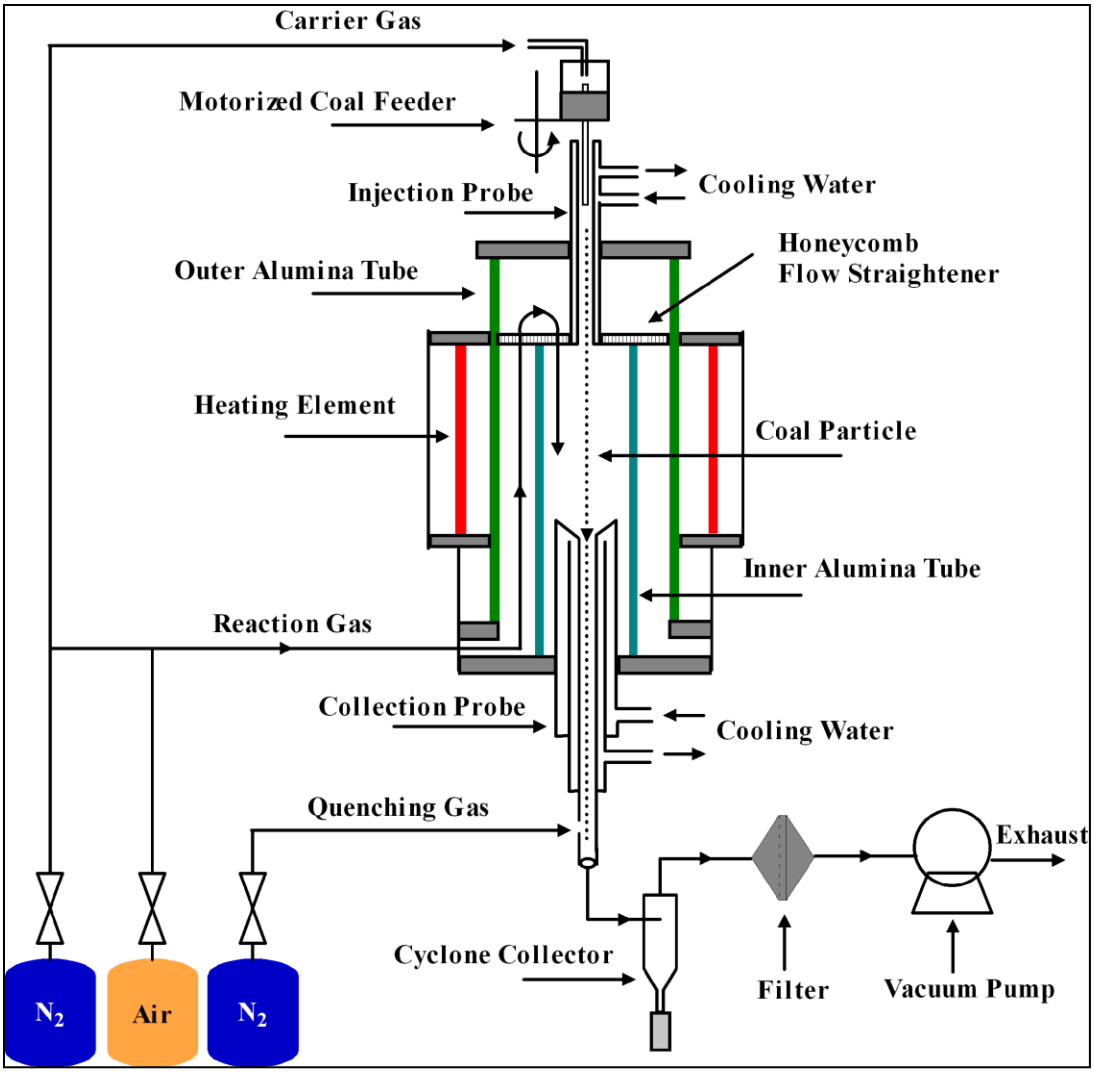

Figure 6: Cross-section view of the laminar entrained-flow reactor

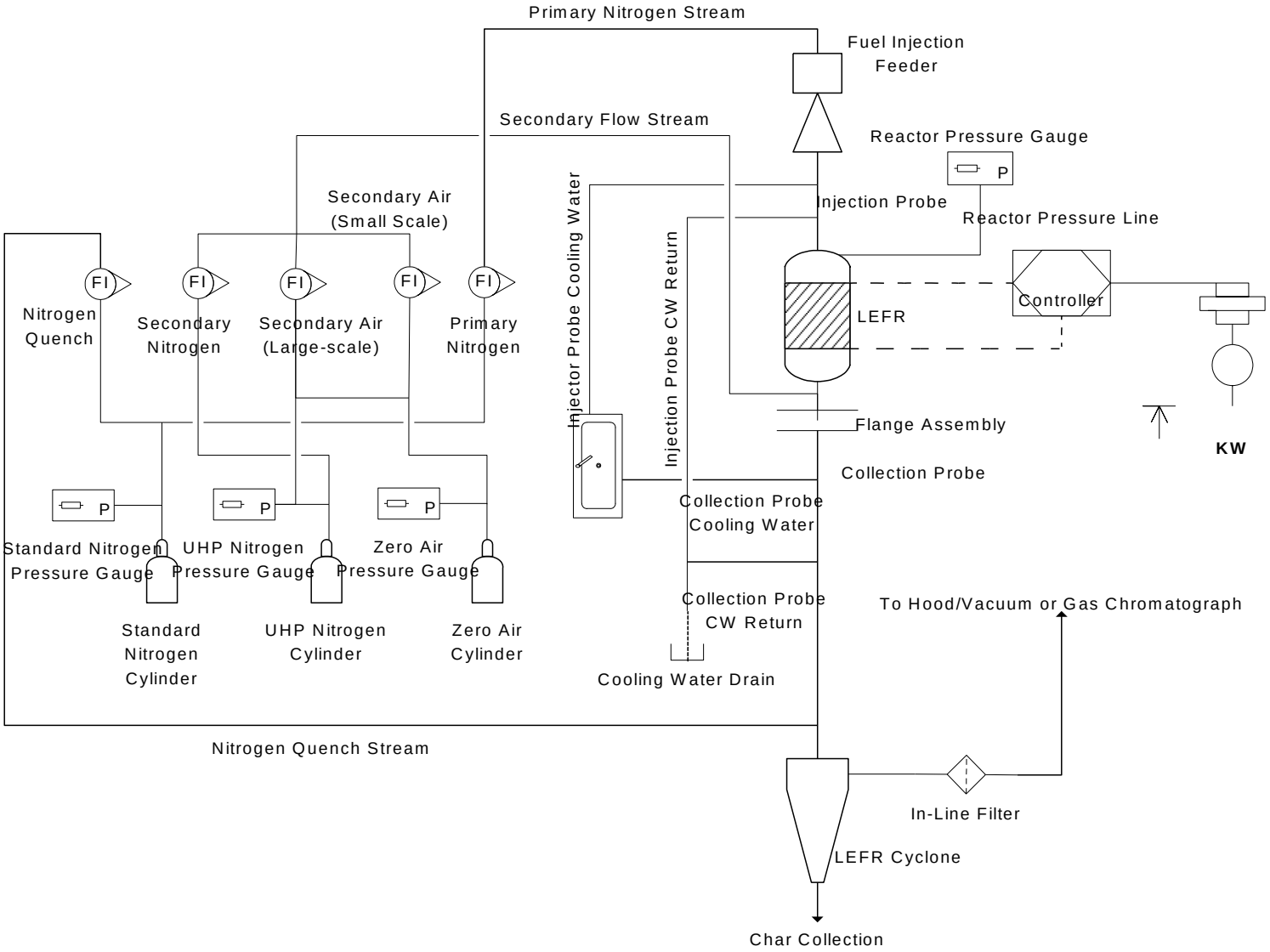

Figure 7: Schematic of the laminar entrained-flow reactor

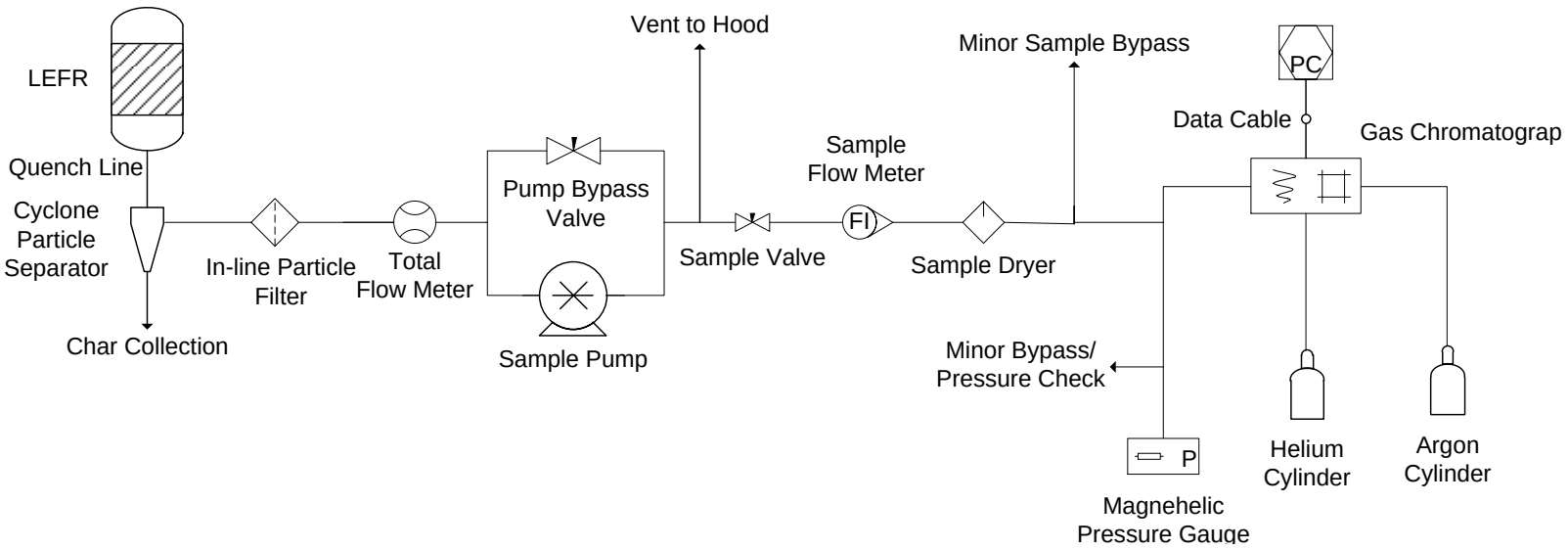

Figure 8: Sampling system schematic with gas chromatograph

Figure 8 shows the LEFR and all subsequent sampling instrumentation; the in-line filter is the same as in Figure 7 and Figure 6. A total flow meter is used to ensure plugs do not form in the system and the pump bypass is used to maintain a constant pressure on the LEFR as well as control the suction head of the pump. The flow vents to a fume hood controlled by a needle valve and flow meter before entering a drierite-containing dryer. The sample gas flow then continues to a tee directly in front of the gas chromatograph sample inlet. A stagnant gas sample is avoided at the inlet of the GC by means of another bypass back to the fume hood; this also allows for a continuous pressure reading as flow passes through the system. It is assumed that the gas has reached room temperature (~25 ℃) by the time it reaches the GC, but the gauge pressure is kept at 1.0 inches of water column using the Magnehelic pressure gauge at the entrance of the GC to ensure constant sampling conditions. The gas chromatograph is manufactured by Varian, model CP-4900, using helium and argon as carrier gases, and is under a class titled microgas chromatographs.

3.1.2.2 Muffle Furnace – Char Yield Determination

This section adds to the validity of using the ash tracer method discussed above. The muffle furnace was manufactured by Blue M Electric Company, 120 V, single phase, with a 50-60 cycle AC, and maximum power of 2 kilowatts; model number M-25A-1A. The system was modified by installing an Omega Engineering temperature controller of model number CN3910AKF.

Using ASTM standards as a reference point[19], the furnace was heated to 850 ℃ to determine the remainder of nonash matter as seen in Figure 4. The operating procedure is as follows:

1. Preheat the furnace to 850 ℃ and clean sample crucibles.

2. Weigh the empty sample crucible and record the weight, then add sample char and record new weight. Do not tare the empty crucible.

3. Place the samples in the muffle furnace and record time of day.

4. After six hours, remove the crucible(s) from the furnace and allow them to reach room temperature.

5. Once cooled, weigh the crucible and char sample and record the weight.

6. Calculate the percent of material evolved by the following equation:

$$\%\ Evolved = \frac{Initial\ Char\ Weight - Final\ Char\ Weight}{Initial\ Char\ Weight}$$

where the initial and final fuel weights are defined:

$$Initial\ Char\ Weight = Initial\ Crucible\ and\ Sample\ Weight - Crucible\ Weight$$

$$Final\ Char\ Weight = Final\ Crucible\ and\ Sample\ Weight - Crucible\ Weight$$

7. Calculate the percent remaining and subsequent char yield as follows:

$$\%\ Remaining = 1 - \%\ Evolved$$

$$Char\ yield = \frac{Ash\ \%\ of\ Char}{\%\ Remaining}$$

Here, the percent remaining is equal to the percentage of ash in the char sample, almost identical to the equation found in the Experimental Approach, above. With this method, both char and volatile yields are quantified.

3.1.2.3 Loss-on-Ignition (LOI)

As per the Scope of Work, loss-on-ignition tests were performed for all chars at 1400 ℃. The procedure is as follows:

1. Heat the hot-foil boat at test conditions to burn off any oils or particles and record weight of boat after ignition cycle is over.
2. Add no more than 0.05 grams of char sample to the boat or some may not burn off when testing begins. The boats have a tendency to close up at the top.
3. Begin test of char sample and record weight of boat and sample when test is over.
4. Calculate percent lost-on-ignition (%LOI) using the following equation.

$$\%\ LOI = \frac{Initial\ Char\ Weight - Final\ Char\ Weight}{Initial\ Char\ Weight}$$

where the initial and final char weights are:

$$Initial\ Char\ Weight = Initial\ Boat\ and\ Sample\ Weight - Boat\ Weight$$

$$Final\ Char\ Weight = Final\ Boat\ and\ Sample\ Weight - Boat\ Weight$$

3.2 Pressurized Wire-Mesh Heater Studies

3.2.1 Experimental Approach

A Design of Experiments (DoE) plan was proposed because four factors were chosen, each at three levels. The factors chosen were fuel type, mesh temperature, vessel pressure, and hold time, each with appropriate levels to test varying effects and two or three factor interactions. These factors and levels are presented in Table 8. A consistent heating rate of 1000 ℃/s was used to more closely approximate the environment of an industrial-scale entrained-flow gasifier. Similar to the high temperature, atmospheric pressure tests, this approach indicates which factors are the most influential.

3.2.2 Apparatuses and Procedure

3.2.2.1 Pressure Vessel and Wire-Mesh Fixtures

The pressure vessel that houses the wire-mesh heater is bolted to I-beams, which are then bolted to the floor to offer rigidity to the apparatus and keep it stationary when the flanges are being tightened. Pressures up to 1000 psig are achievable in the pressure vessel fabricated from schedule 40 six-inch stainless steel pipe and 300-pound stainless steel flanges.

Figure 9 shows a top view of the vessel where the mesh is fixed between two copper blocks with setscrews for clamping the mesh in place; no mesh is shown in this photo. The green block at the bottom of the photograph is the thermocouple block that runs to the heat control hardware. The phenolic board is at a fixed height to eliminate the risk of arcing to the vessel shell. Four holes were drilled in the board to allow nitrogen to enter from the bottom and not disrupt the coal sample when pressurizing.

Table 8: Experimental Conditions used for DoE

Factor	**Levels**
Fuel Type	Bituminous Coal, Lignite, Petcoke
Mesh Temperature, ℃	1000, 1100, 1200
Vessel Pressure, psig	0, 300, 900
Hold Time, seconds	1.0, 3.0, 5.0

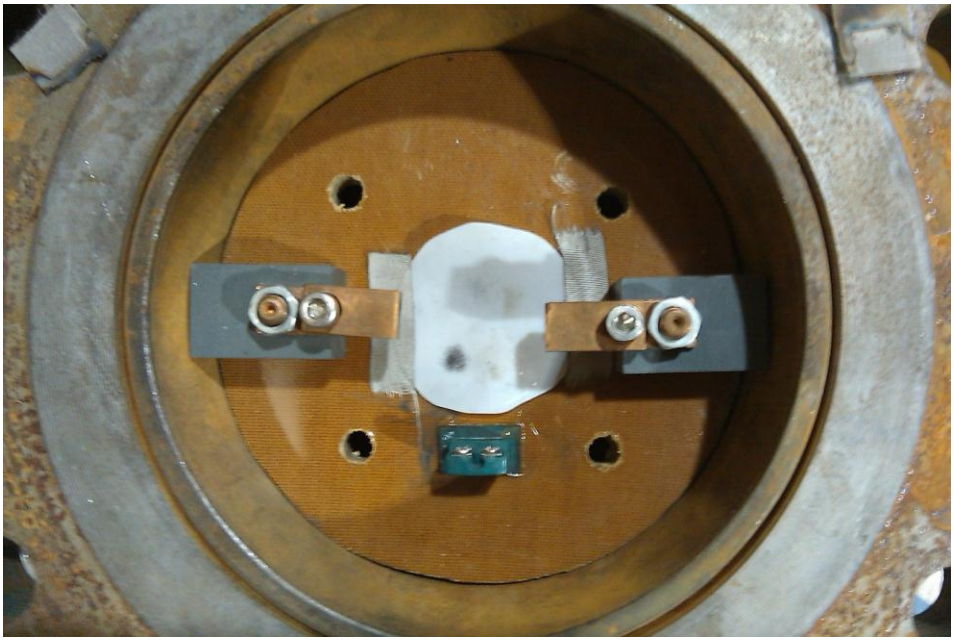

Figure 9: Top view of the grid heater apparatus

Fine-gauge type-R thermocouples were used to accommodate the high temperatures while maintaining a short response time; the bare thermocouples were 0.002 inches in diameter. LabVIEW was used to accomplish a pulse-width modulation (PWM) method of controlling the power output to the mesh without overheating the sample or melting the metal.

Figure 10 shows a photograph of the wire mesh made of 304 stainless steel (SS) with the R-type thermocouple junction. The thermocouples were spot-welded to the mesh using a small dental welder and were cut at 2.0 inch lengths before being attached to the mesh and thermocouple connector. The mesh size for testing was determined to be 2.5 inches long and 1.0 inch wide, which would allow for maximum contact of the mesh to the copper blocks and allow for the mesh to be folded in half lengthwise, thereby securing the fuel within the mesh. A scaled view of the whole mesh is seen in Figure 11.

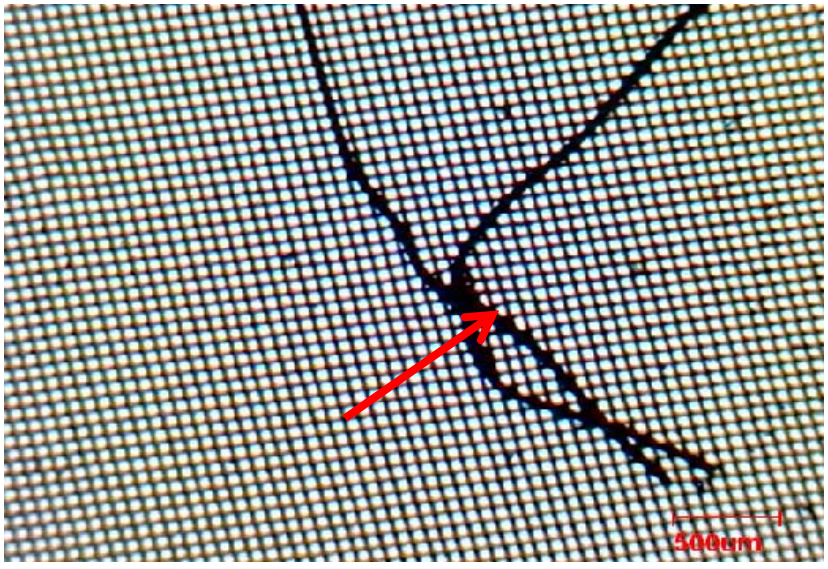

Figure 10: Photograph of the 304 SS wire-mesh and R-type thermocouple leads, scaled. The arrow shows the junction point of the mesh and thermocouple leads.

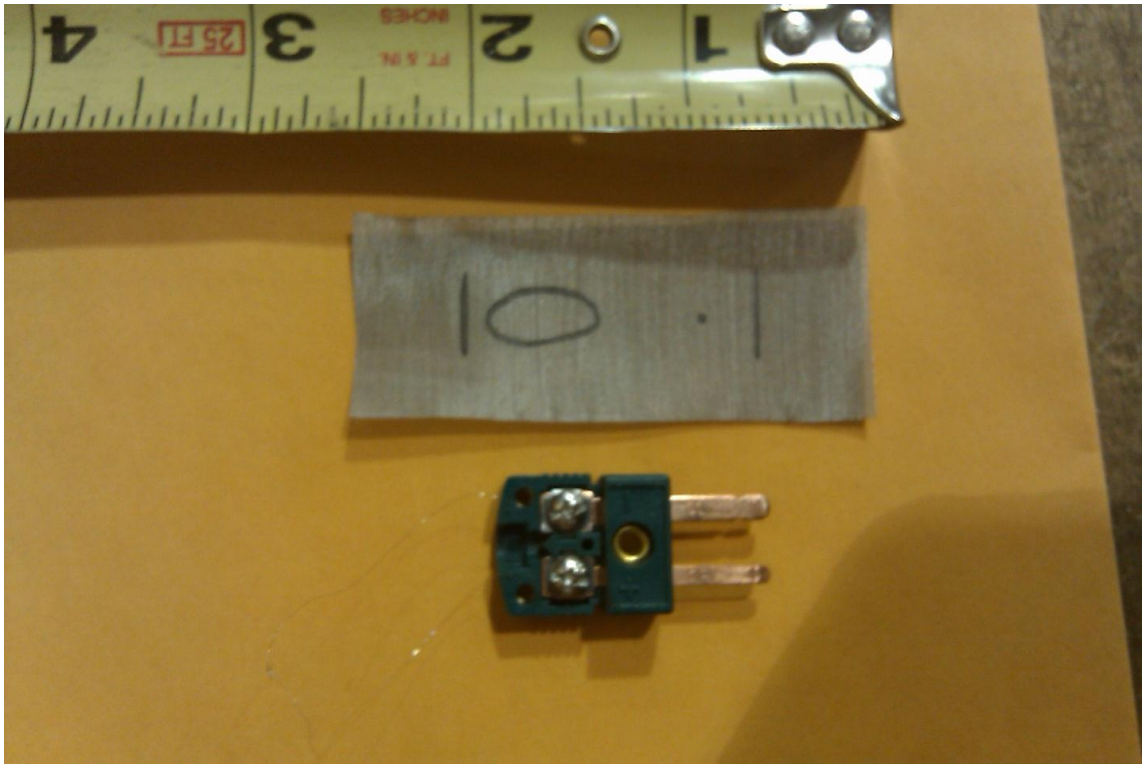

Figure 11: Scaled photograph of the wire mesh and thermocouple connector

3.2.2.2 National Instruments Implementation

To accommodate the high heating rates, National Instruments hardware and software were implemented. The National Instruments hardware consists of two signal-conditioning modules and a central connecting block to interface with LabVIEW version 8.6. Figure 12 shows the signal-conditioning connector box, model SC-2345, and the two signal-conditioning modules for temperature and digital output, models SCC-TC02 and SCC-DO01, respectively. The pulse-width modulation method of controlling the mesh temperature is kept stable via the solid-state relay seen in Figure 13. Here, the wires transmitting the current for heating the mesh (the load) is seen on the left-hand side of the photograph and the control wires are seen at the top right-hand side. These wires come from an AC/DC convertor and the signal-conditioning block.

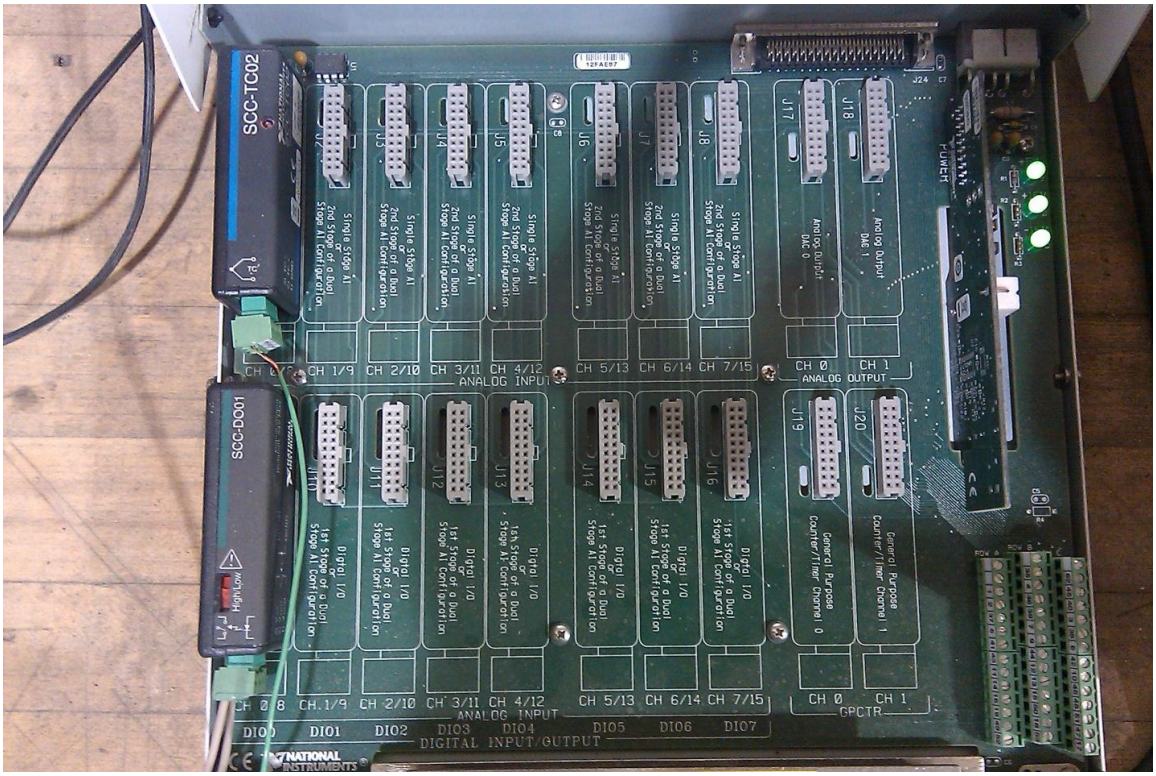

Figure 12: National Instruments signal conditioning block and control modules.

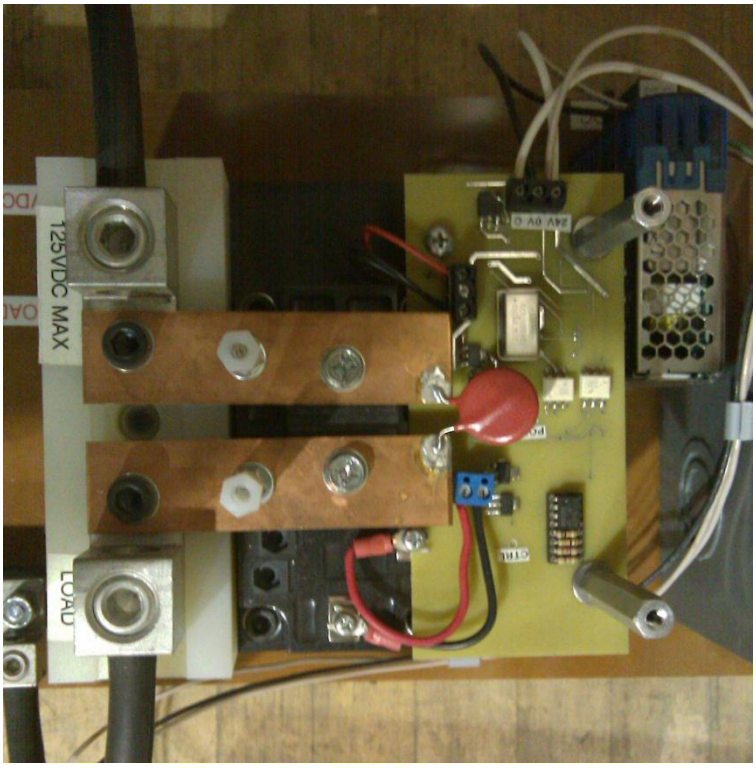

Figure 13: Top view of the solid-state relay used for pulse-width modulation.

A National Instruments LabVIEW-based method of controlling the heating rate and temperature was developed at the University of Utah with the consulting aid of Steve Aposhian of Ingenium Concepts, LLC. The Front Panel display of the LabVIEW interface can be seen in Figure 14. Here, the setpoint profile is designated with appropriate hold times and heating ramps with corresponding temperatures along with file name input for data, pulse-width modulation settings, and PID settings with appropriate gain scheduling for the ramp and soak sections of the setpoint profile.

To validate the heating rate specified by LabVIEW, two lacquers were purchased from Omega Engineering that change color at specified temperatures, model OmegaLAQ. The two lacquers purchased were for 427 °C (800 °F) and 816 °C (1500 °F). Figure 15 shows the lacquer directly applied to the mesh prior to heating and Figure 16

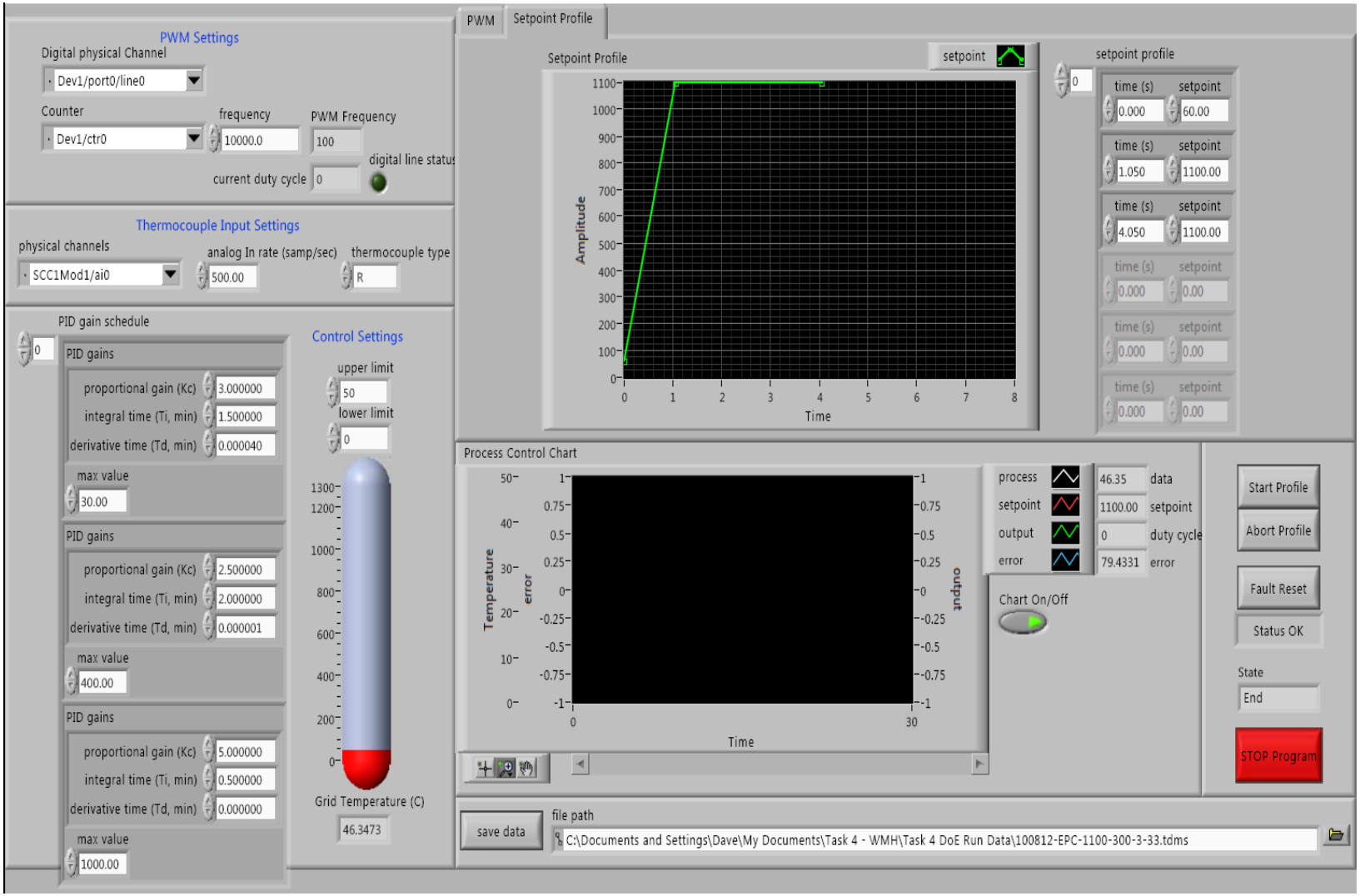

Figure 14: LabVIEW Front Panel display.

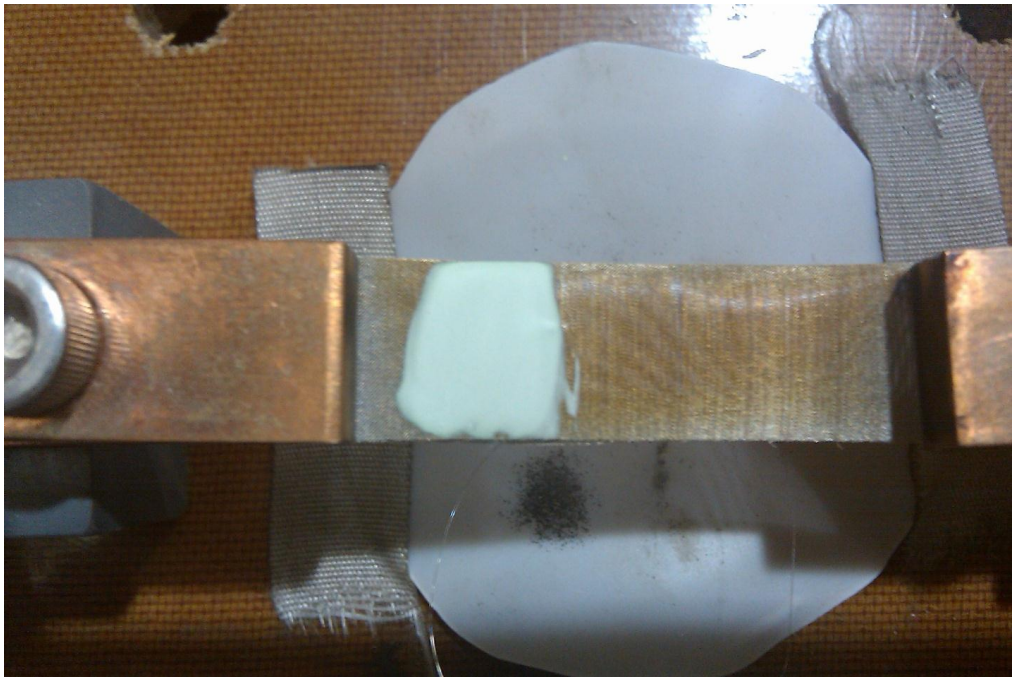

Figure 15: Temperature validation lacquer; before heat is applied.

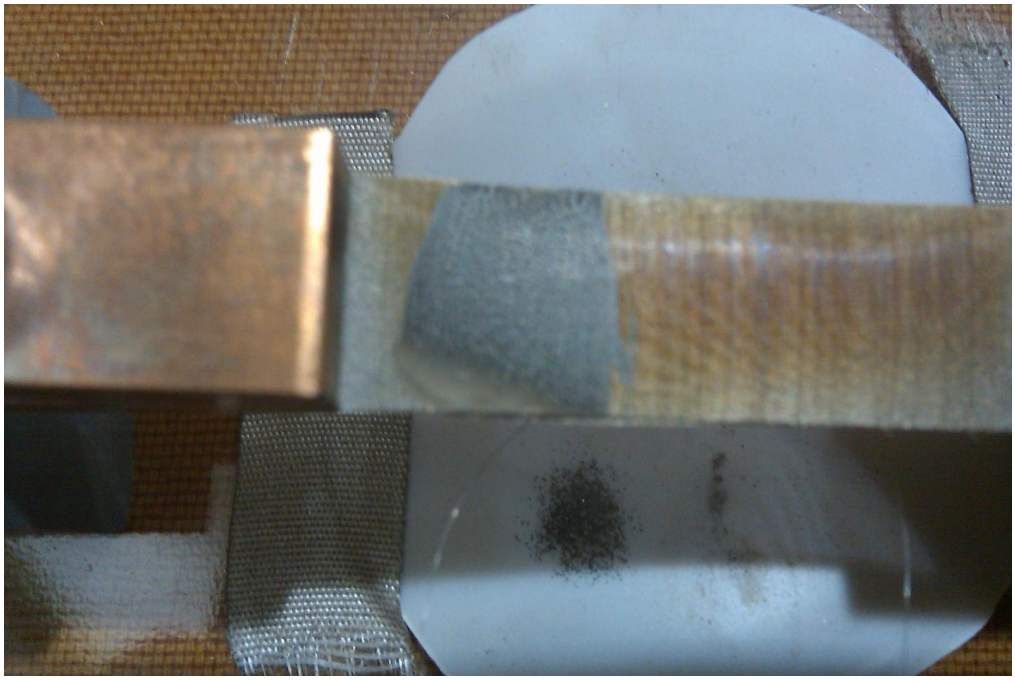

Figure 16: Temperature validation lacquer; after heated at 450 ℃.

shows the mesh after it has been heated to 450 ℃. This validation was performed at the relatively low temperature of 450 ℃ and at the higher temperature of ~800 ℃ to show the path to be linear and not dependent on the PID values and upper limit specified within LabVIEW.

3.2.2.3 Procedure

The operation procedure for the University of Utah's wire-mesh heater is very similar to those of other studies. A mesh is clamped between two conducting plates or jaws and current is run through at a proportional level to achieve a desired temperature with a possible hold time. The apparatus used R-type thermocouples (platinum/rhenium) to accommodate the higher temperatures and were welded to the mesh, ensuring a constant and local temperature reading. Under operation, the fuel was placed on the mesh-thermocouple junction so that the measurement was assured to be the fuel temperature and not just the temperature of the metal. All fuel was sieved to a particle diameter range of 38 to 75 microns. For pressurized operation, the vessel was sealed and nitrogen was run through the system to ensure no oxygen was present; this was verified with a gas chromatograph, manufacturer and model: Varian micro-GC CP4900. The vessel was then slowly pressurized at about six bar per minute to the desired pressure and allowed to rest until the thermocouple measurement fluctuations tapered off according to the LabVIEW interface. Within this interface, desired final temperatures, hold times, and heating rates were specified; a consistent heating rate of 1000 ℃/s was used for all runs. After the test was complete, the pressure was slowly released via a needle valve and the char yield was measured.

A schematic of the entire experimental setup is seen in Figure 17 where the SC-2345 computer module is a National Instruments signal-conditioning box with thermocouple and digital output modules SCC-TC02 and SCC-DO01, respectively.

3.3 Sample Properties

3.3.1 Summary of Methods and Analyses

This section lays out the methods used by different laboratories for sample analysis. It covers the variety of ASTM methods used for ultimate and proximate analyses as well as BTU value and ash composition. Methods for BET surface area, density, and noncomposition ash properties are also discussed, but do not adhere to ASTM standards.

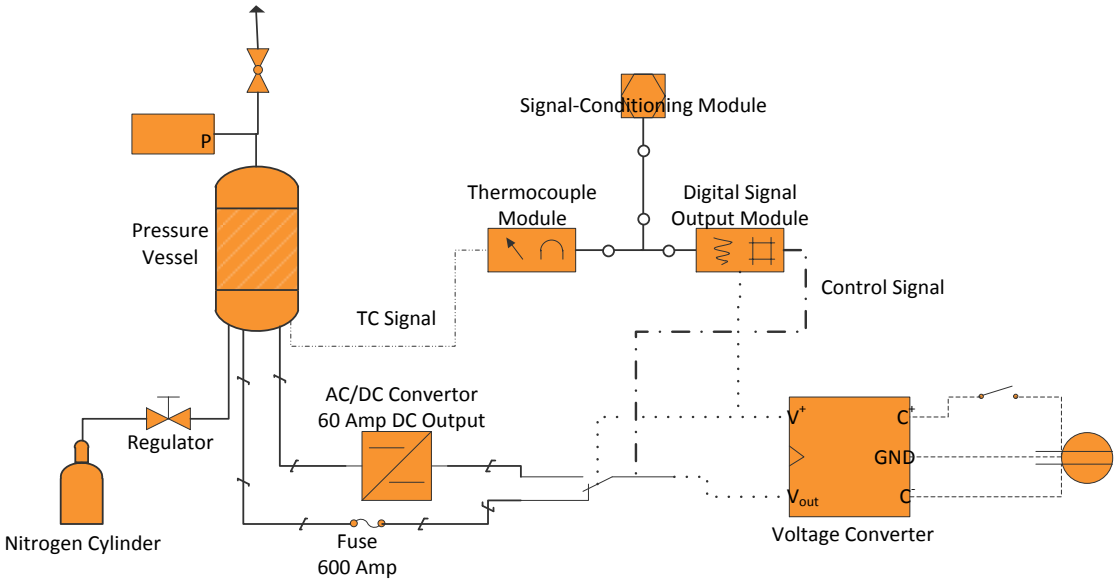

Figure 17: Schematic of the wire-mesh heater experimental apparatus.

3.3.1.1 ASTM and Analytical Methods

3.3.1.1.1 Ultimate Analysis

Here, the percentages of carbon, hydrogen, nitrogen, oxygen, and sulfur are determined on a mass basis[15]. To determine the percentages of these elements, the University of Utah sent samples to Huffman Laboratories in Golden, CO, for analysis and Eastman Chemical Company sent samples to SGS North America Inc. Table 9 shows the ASTM methods used and the corresponding results between the two labs for Appalachian coal to show comparative levels with all other data.

3.3.1.1.2 Proximate Analysis

Percentages of moisture, ash, volatile material, and fixed carbon are included in a proximate analysis[15]. The same laboratories were used for these analyses, SGS and Huffman Labs. These data are contained in Table 9, showing the ASTM methods used.

3.3.1.1.3 Heating Value (BTU Value)

Also called 'calorific value,' this analysis was performed using the same ASTM method of D5865 by both SGS and Huffman Laboratories. The discrepancy on a dry basis for the heating value is only 2.68%.

3.3.1.1.4 Ash Composition

Again, the two laboratories used for this analysis were SGS and Huffman Labs with respect to Appalachian coal. SGS Labs used ASTM D3682, whereas Huffman Lab used ASTM D3174. Table 9 shows the major ash species present and values from both labs for the bituminous coal sample along with the Texas lignite and Eastman petcoke.

Table 9: All tested chemical properties of all sampled fuels

Fuel Sample†			APP			TXL		EPC		Old PC		Method⊗	
Sample Barrel‡			1	10	10	1	10	1	8	1	6		
Ultimate	C (%)	AR*	75.13	76.27	74.31	43.36	42.56	86.86	86.86	82.36	79.71	D5373	D5373
		D	76.24	77.24	75.31	57.44	51.97	87.43	87.4	84.73	83.11		
	H (%)	AR	5.18	5.16	5.06	5.6	4.91	3.65	3.59	3.16	2.94	D5373	D5373
		D	5.09	5.08	5.13	3.79	3.52	3.6	3.54	2.93	2.59		
	N (%)	AR	1.35	1.37	1.45	0.9	0.9	1.7	1.7	1.31	1.27	D5373	D5373
		D	1.36	1.39	1.47	1.19	1.1	1.71	1.71	1.35	1.32		
	O (%)	AR	7.93	7.73	7.01	30.18	28.06	1.66	1.62	2.55	3.98	D5622	D5373 (diff)
		D	6.74	6.7	7.1	11.14	14.62	1.09	1.08	<0.10	0.36		
	S (%)	AR	2.79	2.76	2.79	0.77	0.91	6.45	6.37	5.92	5.37	D4239	D4239 (B)
		D	2.83	2.79	2.83	1.02	1.11	6.49	6.41	6.09	5.60		
Proximate	LOD	AR	1.45	1.25	1.33	24.51	18.11	0.65	0.62	2.80	4.09	D3172	D3302
	Ash (%)	AR	8.57	7.98	8.05	19.3	26.31	0.63	0.68	5.44	6.78	D3172	D3174
		D	8.7	8.08	8.16	25.57	32.13	0.63	0.68	5.60	7.07		
	VM (%)	AR	35.86	35.29	40.06	28.8	27.8	9.41	9.66	8.04	7.61	D3175	D3175
		D	36.39	35.74	40.59	38.15	33.95	9.47	9.72	8.27	7.93		
	Fixed C (%)	AR	54.12	55.48	50.56	27.39	27.78	89.31	89.04	83.72	81.52	D3172	D3172 (diff)
		D	53.46	54.93	51.25	11.77	15.81	89.24	88.98	83.33	80.91		

Table 9: Continued

Fuel Sample†			APP			TXL		EPC		Old PC		Method⊗	
Sample Barrel‡			1	10	10	1	10	1	8	1	6		
Ash Composition (%) of Ash		Al as Al_2O_3	-	22.48	22.5	-	17.27	-	-	-	27.99	D3174	D3682
		Ca as CaO	-	2.75	2.52	-	5.46	-	-	-	7.06	D3174	D3682
		Fe as Fe_2O_3	-	30.05	28.9	-	7.08	-	-	-	10.39	D3174	D3682
		K as K_2O	-	2.35	2.91	-	1.91	-	-	-	1.20	D3174	D3682
		Mg as MgO	-	1.05	0.57	-	1.46	-	-	-	0.71	D3174	D3682
		Mn as MnO	-	0.02	0.05	-	0.05	-	-	-	0.06	D3174	D3682
		Na as Na_2O	-	0.53	0.07	-	0.23	-	-	-	0.59	D3174	D3682
		P as P_2O_5	-	0.04	0.07	-	0.03	-	-	-	0.88	D3174	D3682
		Si as SiO_2	-	37.82	39.2	-	55.61	-	-	-	35.92	D3174	D3682
		Ti as TiO_2	-	1.17	1.12	-	0.99	-	-	-	0.75	D3174	D3682
		S as SO_3	-	3.45	1.22	-	5.99	-	-	-	3.57	D3174	D3682
		BaO	-	-	0.19	-	-	-	-	-	-	-	D3682
		SrO	-	-	0.25	-	-	-	-	-	-	-	D3682
		Undetermined	-	-	0.43	-	-	-	-	-	-	-	D3682
Mercury and Sulfur Forms	Mercury (µg/g)	AR	-	0.14	0.14	-	0.35	<0.005	<0.005	-	<0.01	D6722	D6722
	SO_4 as S * (%)	AR	-	0.08	<0.01	-	0.2	0.23	0.18	-	0.54	D2492	D2492
	Pyritic S (%)	AR	-	1.63	1.46	-	0.39	0.11	<0.10	-	0.19	D2492	D2492
	Organic S (%)	AR	-	1.05	1.32	-	0.33	6.11	6.27	-	4.64	D2492	D2492

* As Received (AR) or Dry (D) basis

† APP – Appalachian Coal, TXL – Texas Lignite, EPC – Eastman Petcoke, Old PC – Previous (initial) lot of Petcoke

‡ Color BLUE denotes Huffman Laboratories; color GREEN denotes SGS Laboratories

⊗ Denotes specified method is ASTM method, unless otherwise stated

From Table 9, there are some significant differences in the constituent values. However, the contribution to these differences from using different ASTM methods is not known. It is important to note that Table 9 displays percentages of ash content; in other words, silicon dioxide constitutes 39.20% of 8.05% of the fuel, according to the SGS Labs data.

3.3.1.1.5 Additional Analytical Analyses

Within the original Scope of Work, ultimate, proximate, heating value, and ash composition analyses were specified, but additional tests were undertaken as well in order to acquire quality information to augment the originally stipulated characterizations. These analyses include sulfur forms, mercury, and other ash-type analyses. Table 9 displays the ASTM methods and comparative values for these additional analyses.

3.3.1.2 Bulk Density

This analysis was performed at the University of Utah for all three key fuels, Appalachian coal, Texas lignite, and the Eastman petcoke. Three different methods were used to give a range of available densities. While all analyses were performed with a 10 cubic centimeter graduated cylinder, the first set was performed with no packing, leaving only gravitational effects. Resulting densities exhibit the lowest practical value seen with a respective fuel. The next set of tests was performed with a moderate amount of tapping the graduated cylinder on a hard surface, allowing for a reasonable level of particle packing; this exhibits a midlevel estimate of bulk density. The third and final set was

performed with a maximum amount of packing, minimizing the void fraction in the cylinder by packing the fuel with a small plunger.

3.3.1.3 Skeletal Density

Since skeletal density is more arduous to measure than bulk density, the University of Utah had samples sent to Micromeritics Analytical Services in Norcross, Georgia. This facility did not use a specific ASTM method, but a strict procedure of purging the sample ten times and calculating skeletal density along with individual deviation, later used to calculate a standard deviation. The principle method used was helium pycnometry, where a sample is weighed and subjected to a helium environment of variable volume. Helium diffuses into the pore structure of the particle, fuel in this case, and the total volume of helium is recorded with respect to temperature and pressure. The particle mass is then divided by the displaced volume, yielding skeletal density.

3.3.1.4 Brunauer, Emmett, and Teller (BET) Surface Area

No specified ASTM method was followed for these analyses. The method that was followed was the University of Utah's Metallurgical Engineering Department's method that has been consistently used and validated using a Micromeritics brand BET surface area analyzer, model ASAP 2010.

3.3.1.5 Ash Fusion Temperature

Eastman Chemical Company conducted these analyses, in which cones of ash were constructed and subjected to increases in temperature, recording any geometrical changes as time progressed. Four distinct temperatures exist for ash fusion analysis:

initial deformation temperature (IT), softening (or spherical) temperature (ST), hemispherical temperature (HT), and fluid temperature (FT). These occurrences are the point at which the cone begins to round, where the base of the cone is equal to its height, the base of the cone is twice its height, and where the cone has spread to a fused mass ≤ 1.6 mm in height, respectively. This method comes from Wayne Ollis of Eastman Chemical Company who conducted these analyses.

3.3.1.6 Ash Viscosity

Eastman Chemical Company conducted these analyses at their Kingsport facility. The method used was the same for both the Appalachian coal and Texas lignite samples, with minor differences in heating rate and final temperature. The method used 72 grams of coal ash charged in a ceramic beaker and placed in a viscometer chamber evacuated of air. A mixed stream of carbon monoxide and carbon dioxide was bled to the chamber to achieve atmospheric pressure and heated at 1.4 ℃/min to a final temperature of 1500 ℃ for the lignite, and 1.7 ℃/min with a final temperature of 1450 ℃ for the bituminous coal (Appalachian). The viscosity measurement was performed under a 4℃/min cooling rate once the final temperatures were achieved for both fuels. No ash viscosity measurements were made for the petcoke given the low ash content of the material.

3.3.1.7 Slurry Stability

Only Texas lignite and Appalachian coal slurry stability tests were conducted. As per Wayne Ollis' method, 2070 grams of as-received coal was weighed in a large beaker, followed by charging it with 918 grams of water and mixing in 12 grams of 50% Tembec ALS (EX-297-012). This yields 0.2% active ALS in the slurry, with a total solids content

of 69%. The solution was then mixed together with an overhead agitator and raised to a pH of 8.0 with 29% ammonium hydroxide.

For the Appalachian coal, the viscosity was incredibly high. Water was carefully added, diluting the solids by 2% increments. Finally, at 62% coal, a reasonable viscosity material was achieved; it is important to note that viscosity was by no means maximized. Then, 338 grams of water was added to obtain a level at which the Kingsport facility would normally run. Ammonia was then added to bring the pH from a value of 7 to a pH of 8. It did not seem to have much effect on the viscosity, qualitatively speaking. A similar analysis was performed for the Texas lignite with the exception that the pH had to be brought up from a value of 5.8 to 8.

3.3.1.8 Thermogravimetric Analysis (TGA)

A TA Instruments Q5000ir was used to generate the TGA data for the as-received samples. Temperature calibration was performed using Alumel (163.0°C), Nickel (359.26°C), Perkalloy (596.0°C), and Iron (780.0°C). Experiments used a nominal sample mass of 10.0 mg in an attempt to minimize the rate of TGA "contamination" attributed to condensing materials, e.g., tars. A heating rate of 5.0°C/min was used to get to a final temperature of 950°C. Heating was conducted in the presence of dry nitrogen purged at 50 cc/min. The data were analyzed using the Universal Analysis 2000 software package of TA Instruments, Version 4.3A. All samples were analyzed at least twice in order to give some sense (both qualitatively and quantitatively) for the variability in the measurement system. The normal practice was to analyze the samples in duplicate, i.e., run TGA on two samples from each mother lot (Fanning, 2009).

3.3.2 Chemical and Physical Fuel Results

Results for the conducted analyses are presented in two tables, one for chemical properties and the other for physical properties. The analyses of the four fuels from five different laboratories are presented in this section. ASTM and varying methods are also specified within respective tables.

Figure 18 shows all TGA-determined solid fuel volatile matter as a function of solid fuel type, solid fuel batch, analysis set, and barrel number from which the sample was taken. From Figure 18, minimal change is seen between barrels or batches of petcoke with respect to volatile matter. In fact, when the totality of the TGA data are considered, it is concluded that there is (essentially) no statistical difference between the original and replacement lots of petcoke, at least from a TGA perspective. Table 10 contains the values from which Figure 18 was generated with corresponding fuel batches, and run dates including applicable analysis sets.

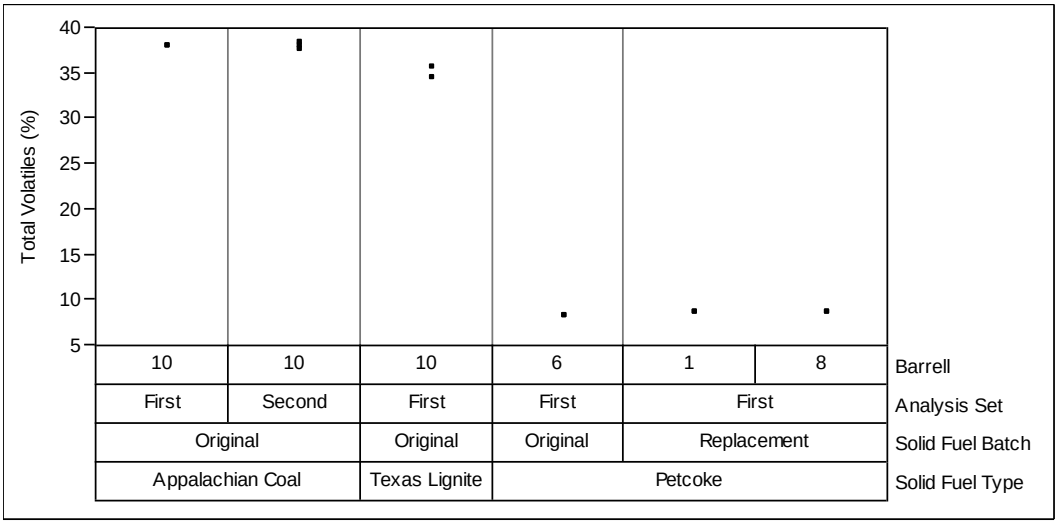

Figure 18: Volatile matter comparison of original solid fuels and selected replacement fuels

Table 10: Thermogravimetric analysis data for volatiles yield

Solid Fuel Type	Solid Fuel Batch	Barrel	Analysis Set	No.	Run Date	Mass (mg)	Total Volatiles (%)
APP	Orig.	10	First	1	4/8/09	10.182	37.80
APP	Orig.	10	First	2	4/9/09	10.443	37.78
APP	Orig.	10	Second	1	4/14/09	10.667	38.31
APP	Orig.	10	Second	2	4/14/09	11.006	37.53
APP	Orig.	10	Second	3	4/14/09	10.827	37.82
TXL	Orig.	10	First	1	4/8/09	9.338	35.45
TXL	Orig.	10	First	2	4/9/09	9.321	34.28
EPC	Rep.	1	First	1	8/19/09	10.959	8.52
EPC	Rep.	1	First	2	8/20/09	10.632	8.42
EPC	Rep.	8	First	1	8/19/09	10.020	8.52
EPC	Rep.	8	First	2	8/20/09	11.438	8.55
OPC	Orig.	6	First	1	4/8/09	10.292	8.19
OPC	Orig.	6	First	2	4/9/09	10.346	8.06

For Barrel 10 of both the Appalachian coal and Texas lignite, ash viscosity curves are presented in Figure 19 and Figure 20. Figure 20 is a logarithmic plot of the viscosity data.

It is important to note that the spikes on the Texas lignite ash viscosity profile do not rise from the sample itself. (The spikes on the Appalachian coal profile are much smaller.) Mike Brannon of Eastman Chemical Company said they stem from the software having to periodically readjust the speed of the viscometer to not exceed the equipment's maximum torque specifications. In effect, the data acquisition software decreases the speed by 0.1 RPM to keep the torque within an appropriate range.

Figure 21 offers a comparison from the Kirk-Othmer Encyclopedia of Chemical Technology. Shown in the ash viscosity-temperature plot are two pertinent coals, Blacksville (Appalachian) and Drayton, a bituminous coal. This reference indicates that the variability of two similar ranked coals can have a large difference in viscosity profiles.

Since the EPC proximate analysis shows less than 1.0% ash, subsequent testing of ash viscosity and ash fusion temperatures were not pursued given the effort and amount of raw petcoke that would be required to prepare a sufficient quantity of ash for testing. It is also important to note that the solid fuel EPC petcoke was not the first petcoke sample studied. Prior testing was performed on a fuel that was found to have an ash content of 5.6-7.1%; this is titled the Old PC in Table 9 and Table 11. In light of the abnormally high ash content, Eastman Chemical Company and the University of Utah jointly decided to find another lot of petcoke having an ash content more representative of a "typical" petcoke. The replacement material is identified as EPC petcoke.

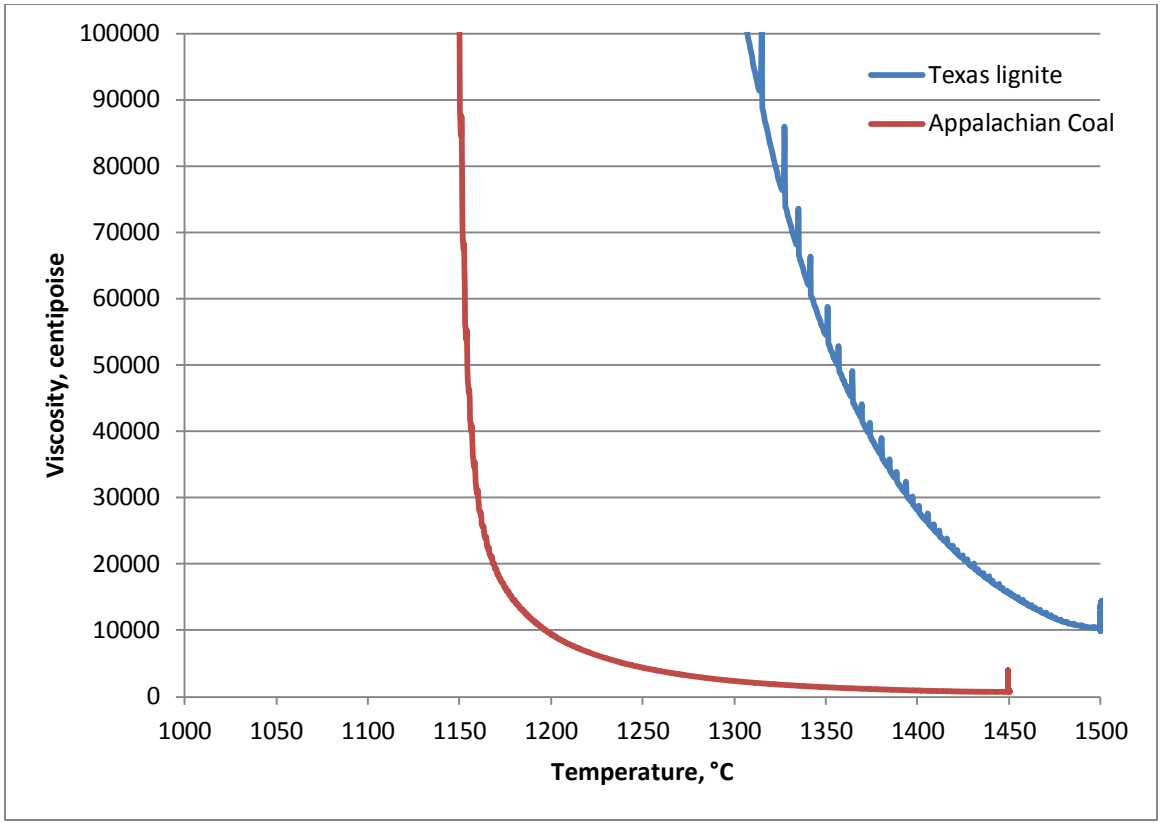

Figure 19: Comparison plot of Appalachian bituminous coal and Texas lignite ash viscosities

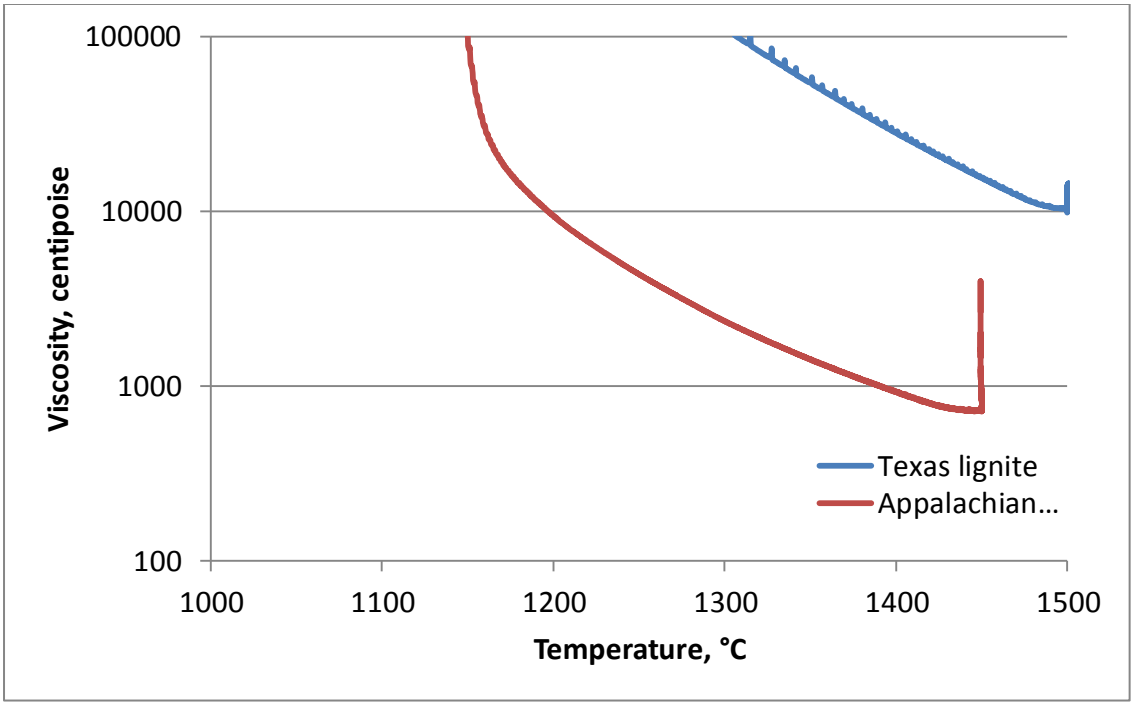

Figure 20: Log plot of Appalachian bituminous coal and Texas lignite ash viscosities

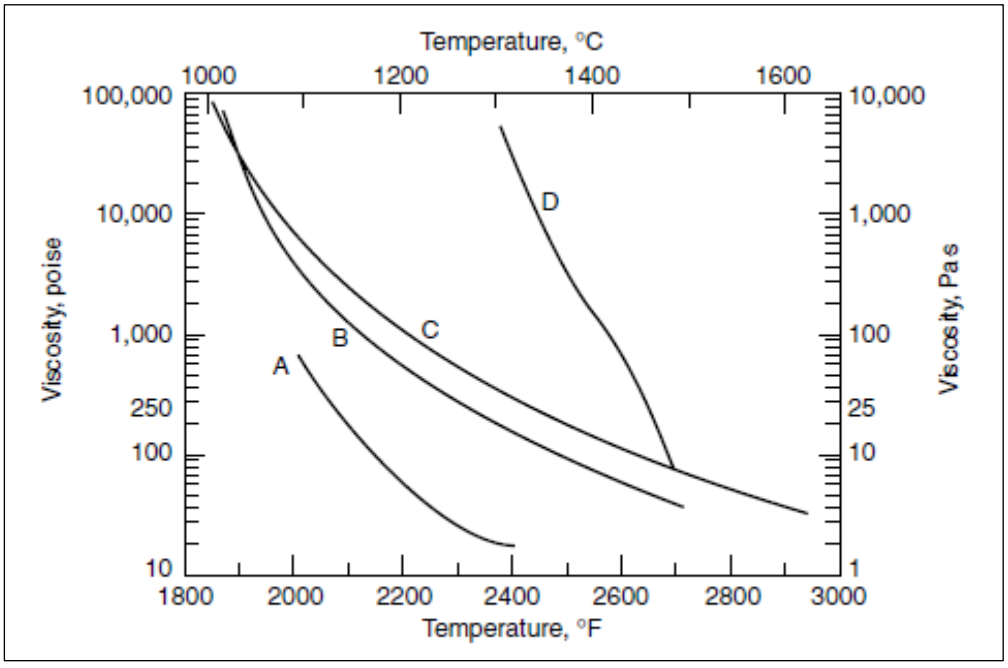

Figure 21: Coal ash viscosity-temperature profiles of (A) Buckskin (B) Pyro No. 9 (C) Blacksville (Appalachia) and (D) Drayton (bituminous); [3].

Table 11: All tested physical properties of all sampled fuels

Fuel Sample			APP			TXL		EPC		Old PC		Method⊗	
Sample Barrel			1	10	10	1	10	1	8	1	6		
Heating Value (Btu/lb)		AR*	13632	13807	13427	7234	7125	14981	14984	13781	13351	D5865	D5865
		D	13833	13982	13607	9583	8701	15079	15077	14178	13920		
Bulk Density	Lightly Packed (g/cm^3)	Value	-	0.44	-	-	0.464	-	0.557	-	-	U of U	
		St. Dev.	-	0.0074	-	-	0.004	-	0.0032	-	-		
	Heavily Packed (g/cm^3)	Value	-	0.725	-	-	0.802	-	0.799	-	-		
		St. Dev.	-	0.0029	-	-	0.0077	-	0.0126	-	-		
Skeletal Density (g/cm^3)		Value	-	1.354	-	-	1.485	-	1.407	-	-	MicroM	
		St. Dev.	-	0.0009	-	-	0.0004	-	0.006	-	-		
BET Surface Area (m^2/g)		Value	-	2.088	-	-	5.712	-	8.58	-	-	U of U	
		St. Dev.	-	0.0214	-	-	0.0588	-	0.2315	-	-		
Ash Fusion Temperature (°C)		IT	-	1054	-	-	1133	-	-	-	-	Eastman	
		ST	-	1129	-	-	1182	-	-	-	-		
		HT	-	1281	-	-	1288	-	-	-	-		
		FT	-	1312	-	-	1454	-	-	-	-		
Additional Analytical		Sum of Oxides	-	99.57%	-	-	-	-	-	-	-	D3682	
		Silica Value	-	55.06	-	-	-	-	-	-	-	D3682	
		Base Acid Ratio	-	0.56	-	-	-	-	-	-	-	D3682	
		T250 Temperature	-	2260 °F	-	-	-	-	-	-	-	D3682	
		Fouling Index	-	0.04	-	-	-	-	-	-	-	D3682	
		Slagging Index	-	1.57	-	-	-	-	-	-	-	D3682	
		Type of Ash	-	Bituminous	-	-	-	-	-	-	-	D3682	

* As Received (AR) or Dry (D) basis

† APP – Appalachian Coal, TXL – Texas Lignite, EPC – Eastman Petcoke, Old PC – Previous (initial) lot of Petcoke

‡ Color BLUE denotes Huffman Laboratories; color GREEN denotes SGS Laboratories; color PINK denotes Eastman Labs; color ORANGE denotes University of Utah and Micromeritics Laboratories

⊗ Denotes ASTM method, unless specified by a specific laboratory where the method was developed; 'U of U' is the University of Utah and 'MicroM' is Micromeritics

The slurry stability analysis results are presented in Figure 22 and Figure 23 for Appalachian coal and Texas lignite, respectively.

Figure 22 shows the Appalachian coal to be shear-thickening (dilatants), whereas Figure 23 shows the Texas lignite to be shear-thinning, evident of pseudoplastic behavior.

3.3.3 Discussion of Fuel Results

Evaluating the three fuels against one another is not only useful in understanding the properties of each fuel, but such a comparison also facilitates understanding how they each might perform relative to the others in a gasification process. With respect to ash levels, three distinct ranges are given with the three different ranked fuels, very low ash, moderate ash, and high ash levels. The data may also be interpreted as one fuel having low, moderate, or high fixed carbon corresponding to lignite, bituminous coal, and petcoke, respectively. These kinds of relationships for the three fuels could be made

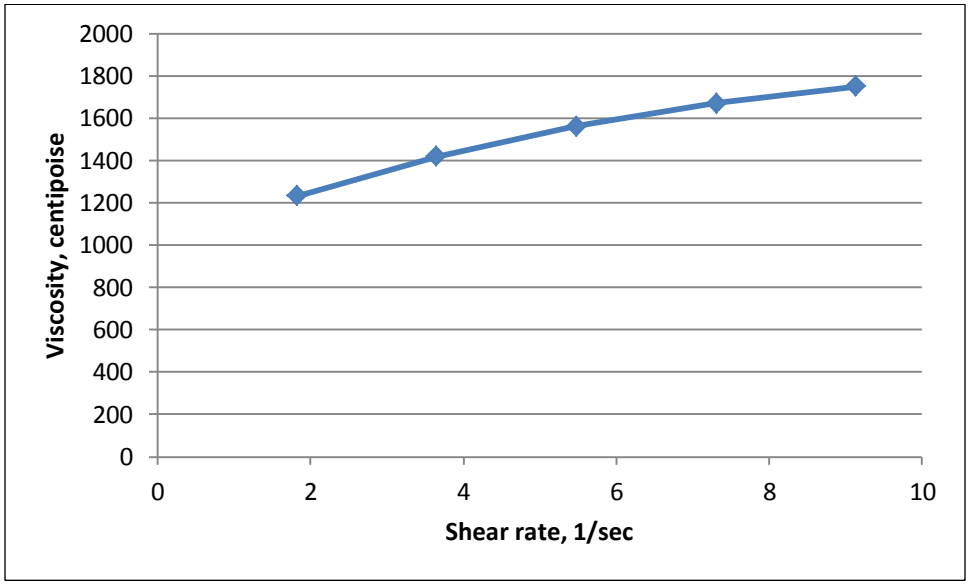

Figure 22: Slurry stability curve for Appalachian coal

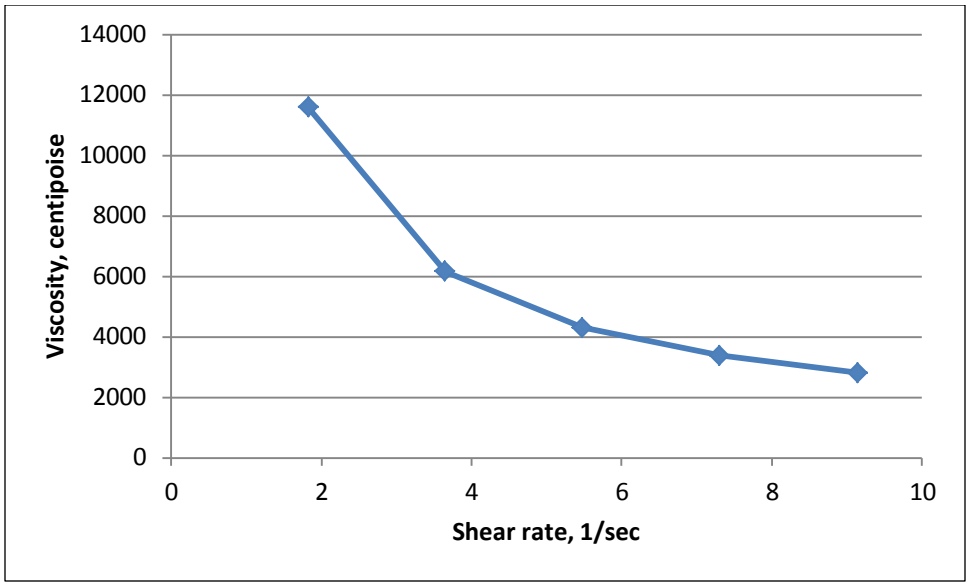

Figure 23: Slurry stability curve for Texas lignite

repeatedly, but many additional considerations become important when choosing a fuel for a gasification process.

Proximate analyses for the fuels, as they vary from first and last barrels, are more inconsistent than the ultimate analyses. The same case could be made for these analyses with respect to calculations and associated error, and still, the lignite samples have the greatest variability. The loss-on-drying value alone changes more than 6% between the first and last barrel, whereas the bituminous coal changes 0.2% and the petcoke (EPC) changes only 0.03%. A case could be made that an impurity was in the lignite prior to or was somehow introduced upon pulverization. If the impurity (trash or soil for instance) was on the top of the lignite when being pulverized, the first barrels would be less precise than the later barrels, or vice versa. In addition to the basic fuel characterization carried out by the different laboratories, thermogravimetric analyses (TGA) were performed on the solid fuels. The proximate and subsequent analytical data have been validated to a

degree because of the generated TGA data. Total volatile yield was measured by thermogravimetric analysis resulting in 34.3% to 35.5% volatile matter, which corresponds well to 33.95% on a dry basis from Huffman Labs.

Ash composition for the three fuels is within reason, but discrepancies exist between Appalachian coal values for Huffman and SGS labs. These differences could stem from the ASTM methods used by each laboratory or might simply reflect the variability in composition within these heterogeneous solid fuels. Even though different methods were used, however, the major constituents of the ash correspond well, especially Al as Al_2O_3, Fe as Fe_2O_3, and Si as SiO_2. Other species could differ not only by ASTM standards, but detection limits as well. Since all species in the ash are below 5%, except for the three mentioned above, the limit could be small resulting in larger error in the value itself. Another view is that some species' influence is not as great as in other fuels. With EPC petcoke, the ash composition values are relatively small compared to the bituminous or lignite coals, which are on the order of 0.5%. Ash composition values for all fuels appear reasonable and within an acceptable range of error.

Physical differences in the tested fuels are seen in Table 11. Here, both skeletal and bulk densities and BET surface areas are given with standard deviation. Lightly and heavily packed scenarios are given for bulk density since there is never one set value. Depending on the void fraction of the storage container or feed hopper, the value of the density will change; it could even change within the vessel from the base to the top and compact with time. The skeletal density, however, takes all helium-permeable pores in the structure into consideration by measuring the total void fraction of the sample. The BET surface area works on a similar permeable principle, but with respect to

physisportion of nitrogen at -196 ℃. The differences in surface areas of the fuels make sense from a practical standpoint and considering the respective fuel ranks. The bituminous coal has the lowest surface area, which could be rationalized because it is the oldest coal and has been exposed to higher pressure for a longer period of time. Texas lignite has the next largest surface area, which is based on the same rational as the bituminous coal. The EPC petcoke has the largest value because it has already been subjected to high temperatures and has lost most of its volatile material, opening more pores and increasing surface area.

Ash fusion temperatures were added to the initial Scope of Work because of the importance in considering ash yields and subsequent thermal behavior, i.e., melting, and fluid behavior of the ash in slagging gasifiers. The difference in the four ash fusion temperature stages of Appalachian coal and Texas lignite likely stem from the higher silicon content of the lignite; it contains about 18% more silicon oxide, thereby melting at higher temperatures. In conjunction with the ash viscosity curves for the two coals, seen in Figure 19 and Figure 20, fluid properties can be calculated and shear stresses identified

CHAPTER 4

RESULTS AND DISCUSSION

4.1 Entrained-Flow Pyrolysis Studies

This section presents the results and corresponding discussion of all char and volatile yields, major gas species concentrations, and loss-on-ignition data.

4.1.1 Char and Volatile Yields

Tabulated below are the char and volatile yield values as per the muffle furnace method described in Section 3.1.2.2 Muffle Furnace – Char Yield Determination. Table 12 presents the respective char and volatile yields for the Appalachian coal (APP), Texas lignite (TXL), and Eastman petcoke (EPC) with corresponding temperature (T) and oxygen to carbon ratio (O/C). The run numbers are the corresponding values as described in Section 3.1.1 Experimental Approach and given in Table 12. Since volatile yields are determined from char yield calculations, discussion will favor the char yield results.

While the table is informative, the following figures allow for a visual representation of the data. Figure 24 displays the char yields versus the O/C ratio at the respective temperatures, showing the range in the repeated runs of 1 and 6 (O/C=1.0 and 1250 ℃). The trends of Figure 24 are inconsistent with what was expected and show that char yield decreases at 1100 ℃ as oxygen percentage increases, but increases with increasing oxygen for temperatures of 1250 ℃. Both trends are seen in ranging oxygen

Table 12: Char and volatiles yields of laminar entrained-flow reactor runs

Fuel	Run No.	Char Yield	Volatiles Yield	T and O/C
APP	1	71.38%	28.62%	1250, 1
APP	2	40.34%	59.66%	1400, 2
APP	3	62.26%	37.74%	1100, 0
APP	4	54.01%	45.99%	1400, 0
APP	5	43.31%	56.69%	1100, 2
APP	6	63.42%	36.58%	1250, 1
APP	7	47.73%	52.27%	1250, 0
APP	8	67.06%	32.94%	1400, 1
EPC	1	58.52%	41.48%	1250, 1
EPC	2	39.52%	60.48%	1400, 2
EPC	3	84.20%	15.80%	1100, 0
EPC	4	57.52%	42.48%	1400, 0
EPC	5	33.10%	66.90%	1100, 2
EPC	6	36.38%	63.62%	1250, 1
EPC	7	46.01%	53.99%	1250, 0
EPC	8	45.38%	54.62%	1400, 1
TXL	1	42.93%	57.07%	1250, 1
TXL	2	30.94%	69.06%	1400, 2
TXL	3	64.95%	35.05%	1100, 0
TXL	4	57.73%	42.27%	1400, 0
TXL	5	43.80%	56.20%	1100, 2
TXL	6	39.82%	60.18%	1250, 1
TXL	7	55.84%	44.16%	1250, 0
TXL	8	38.97%	61.03%	1400, 1

contents at a temperature of 1400 ℃. With an increase in oxygen content, char yields are expected to decrease because more oxygen is available for gasification reactions.

Figure 25 shows the same visual analysis as Figure 24, but for the Eastman petcoke, EPC. The trends are a little more distinguished, but still have a substantial error within the repeated runs at 1250 ℃ and oxygen-to-carbon ratio of one. Figure 26 displays the same analysis as the previous two figures, but for the Texas lignite, TXL. Here, the trends make much more sense on a qualitative level, but are less credible because of the inconsistencies in Figure 24 and the tight distributions displayed in Figure 25 at 1400 ℃. The plot for Texas lignite match what was generally expected; as oxygen content increases, char yield decreases in addition to the range being smaller for repeated runs at O/C=1.0 and 1250 ℃.

The discrepancies in these figures are discussed later with loss-on-ignition (LOI) data and show that the differences in char yields are closely related to the final particle size distribution of the chars and agglomeration of particles.

4.1.2 Major Gas Species Concentrations

A microgas chromatograph was used to record the major gas species that evolved from the pyrolysis and gasification reactions within the laminar entrained-flow reactor for the respective oxygen-to-carbon ratios and temperatures. Carbon monoxide, carbon dioxide, hydrogen, methane, and hydrogen sulfide were the key gas species measured. Table 13, Table 14, and Table 15 display the gas data given in mole percent of product stream with corresponding run number and appropriate O/C and temperature for the three solid fuels.

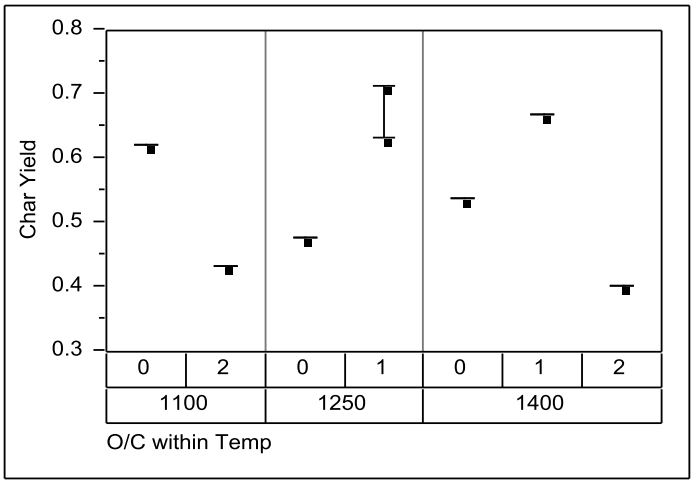

Figure 24: Appalachian coal (APP) char yield as a function of temperature and O/C ratio

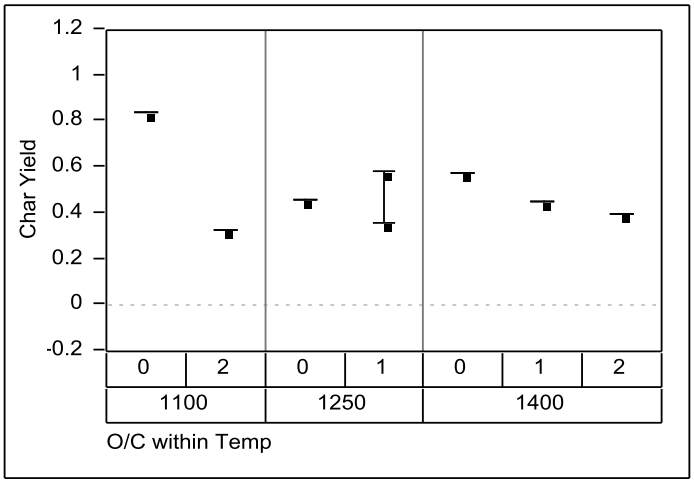

Figure 25: Eastman petcoke (EPC) char yield as a function of temperature and O/C ratio

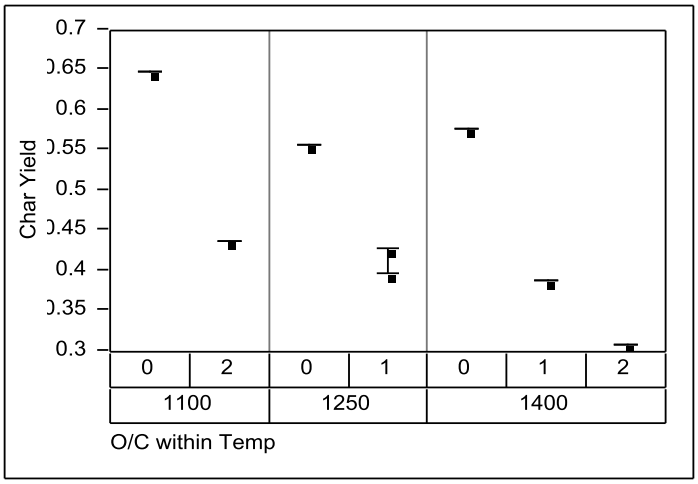

Figure 26: Texas lignite (TXL) char yield as a function of temperature and O/C ratio

Table 13: Major gas-phase species of LEFR tests for Appalachian coal

RUN	Appalachian Coal							
1	**1250°C, O/C=1**							
		CO	CO2	H2	CH4	H2S	Others	Sum
	Average	0.050	0.643	0.430	0.020	0.000	0.000	1.143
	St. Dev.	0.0183	0.0443	0.1166	0.0082	0.0000	0.0000	0.1066
2	**1400°C, O/C=2**							
		CO	CO2	H2	CH4	H2S	Others	Sum
	Average	0	1.8875	0.095	0	0	0	1.9825
	St. Dev.	0.0000	0.1486	0.0208	0.0000	0.0000	0.0000	0.1427
3	**1100°C, O/C=0**							
		CO	CO2	H2	CH4	H2S	Others	Sum
	Average	0.2425	0.01	0.5325	0.085	0	0	0.87
	St. Dev.	0.0519	0.0000	0.0877	0.0191	0.0000	0.0000	0.1564
4	**1400°C, O/C=0**							
		CO	CO2	H2	CH4	H2S	Others	Sum
	Average	0.035	0.0025	0.92	0.0125	0	0	0.97
	St. Dev.	0.0238	0.0050	0.1615	0.0096	0.0000	0.0000	0.1896
5	**1100°C, O/C=2**							
		CO	CO2	H2	CH4	H2S	Others	Sum
	Average	0.0125	1.615	0.015	0.005	0	0	1.6475
	St. Dev.	0.0150	0.0404	0.0058	0.0058	0.0000	0.0000	0.0544
6	**1250°C, O/C=1**							
		CO	CO2	H2	CH4	H2S	Others	Sum
	Average	0	0.7175	0.075	0	0	0	0.7925
	St. Dev.	0.0000	0.0386	0.0370	0.0000	0.0000	0.0000	0.0250
7	**1250°C, O/C=0**							
		CO	CO2	H2	CH4	H2S	Others	Sum
	Average	0	0	0.9175	0	0	0	0.9175
	St. Dev.	0.0000	0.0000	0.0457	0.0000	0.0000	0.0000	0.0457
8	**1400°C, O/C=1**							
		CO	CO2	H2	CH4	H2S	Others	Sum
	Average	0	0.5625	0.465	0	0	0	1.0275
	St. Dev.	0.0000	0.0359	0.0580	0.0000	0.0000	0.0000	0.0580

Table 14:Major gas-phase species of LEFR tests for Petcoke

RUN	EPC Petcoke							
1	**1250°C, O/C=1**							
		CO	CO2	H2	CH4	H2S	Others	Sum
	Average	0.000	0.283	0.000	0.000	0.000	0.000	0.283
	St. Dev.	0.0000	0.0050	0.0000	0.0000	0.0000	0.0000	0.0050
2	**1400°C, O/C=2**							
		CO	CO2	H2	CH4	H2S	Others	Sum
	Average	0	0.99	0	0	0	0	0.99
	St. Dev.	0.0000	0.0000	0.0000	0.0000	0.0000	0.0000	0.0000
3	**1100°C, O/C=0**							
		CO	CO2	H2	CH4	H2S	Others	Sum
	Average	0	0	0.2525	0.03	0	0	0.2825
	St. Dev.	0.0000	0.0000	0.0050	0.0000	0.0000	0.0000	0.0050
4	**1400°C, O/C=0**							
		CO	CO2	H2	CH4	H2S	Others	Sum
	Average	0	0	0.5325	0	0	0	0.5325
	St. Dev.	0.0000	0.0000	0.0096	0.0000	0.0000	0.0000	0.0096
5	**1100°C, O/C=2**							
		CO	CO2	H2	CH4	H2S	Others	Sum
	Average	0	0.33	0	0	0	0	0.33
	St. Dev.	0.0000	0.0082	0.0000	0.0000	0.0000	0.0000	0.0082
6	**1250°C, O/C=1**							
		CO	CO2	H2	CH4	H2S	Others	Sum
	Average	0	0.3125	0	0	0	0	0.3125
	St. Dev.	0.0000	0.0236	0.0000	0.0000	0.0000	0.0000	0.0236
7	**1250°C, O/C=0**							
		CO	CO2	H2	CH4	H2S	Others	Sum
	Average	0	0	0.375	0	0	0	0.375
	St. Dev.	0.0000	0.0000	0.0332	0.0000	0.0000	0.0000	0.0332
8	**1400°C, O/C=1**							
		CO	CO2	H2	CH4	H2S	Others	Sum
	Average	0	0.3275	0	0	0	0	0.3275
	St. Dev.	0.0000	0.0126	0.0000	0.0000	0.0000	0.0000	0.0126

Table 15: Major gas-phase species of LEFR tests for Lignite

RUN	Texas Lignite							
1	**1250°C, O/C=1**							
		CO	CO2	H2	CH4	H2S	Others	Sum
	Average	0.000	0.295	0.300	0.000	0.000	0.000	0.595
	St. Dev.	0.0000	0.0058	0.0294	0.0000	0.0000	0.0000	0.0289
2	**1400°C, O/C=2**							
		CO	CO2	H2	CH4	H2S	Others	Sum
	Average	0	0.6275	0.1525	0	0	0	0.78
	St. Dev.	0.0000	0.0096	0.0050	0.0000	0.0000	0.0000	0.0141
3	**1100°C, O/C=0**							
		CO	CO2	H2	CH4	H2S	Others	Sum
	Average	0	0.03	0.235	0.015	0	0	0.28
	St. Dev.	0.0000	0.0000	0.0238	0.0058	0.0000	0.0000	0.0294
4	**1400°C, O/C=0**							
		CO	CO2	H2	CH4	H2S	Others	Sum
	Average	0	0.02	0.6025	0	0	0	0.6225
	St. Dev.	0.0000	0.0000	0.0340	0.0000	0.0000	0.0000	0.0340
5	**1100°C, O/C=2**							
		CO	CO2	H2	CH4	H2S	Others	Sum
	Average	0	0.6275	0.0425	0	0	0	0.67
	St. Dev.	0.0000	0.0287	0.0096	0.0000	0.0000	0.0000	0.0294
6	**1250°C, O/C=1**							
		CO	CO2	H2	CH4	H2S	Others	Sum
	Average	0.005	0.375	0.22	0	0	0	0.6
	St. Dev.	0.0100	0.0058	0.0082	0.0000	0.0000	0.0000	0.0200
7	**1250°C, O/C=0**							
		CO	CO2	H2	CH4	H2S	Others	Sum
	Average	0	0.0325	0.3575	0	0	0	0.39
	St. Dev.	0.0000	0.0050	0.0050	0.0000	0.0000	0.0000	0.0082
8	**1400°C, O/C=1**							
		CO	CO2	H2	CH4	H2S	Others	Sum
	Average	0.0075	0.3125	0.175	0	0	0	0.495
	St. Dev.	0.0096	0.0150	0.0129	0.0000	0.0000	0.0000	0.0265

Given are averages of four gas chromatograph (GC) runs with subsequent standard deviations. In addition to the key gas species, a column denoted by 'others' indicates if any additional species were present; this does not include oxygen and nitrogen present from the inlet or carrier gas streams.

The validity of this data, on a quantitative level, leaves much to be desired. Through statistical analysis, it was determined that no clear relationship could be established between the production of all major gas species. While some gas species trends coincide with the theoretical prediction, others seem erratic to the extent of noise within the instrument. The case for carbon dioxide is an example of when the yields behaved well with clear trends, seen in Figure 27.

Figure 27 displays the mole percent of carbon dioxide with respect to temperature and O/C ratio within specified target values for the Appalachian coal fuel. As temperature increases, CO_2 production increases along with increasing oxygen content, as theory would predict. Three other figures for carbon monoxide, hydrogen, and methane are found in Figure 28, Figure 29, and Figure 30, respectively, for Appalachian coal. The quantitative value of these three figures is much less than for carbon dioxide, Figure 27.

Carbon monoxide evolution is seen in Figure 28 where the only discernable trend is that CO production decreases as temperature is increased for set oxygen content. It is disconcerting that Figure 29 and Figure 30 both exhibit such erratic behavior with respect to the independent variables of oxygen content and temperature. No discernable trends are seen in the figures themselves, unlike Figure 28 and in particular Figure 27. An indication of inter-species-dependency as a qualitative means to explain major gas species during Appalachian coal testing is found in Figure 31.

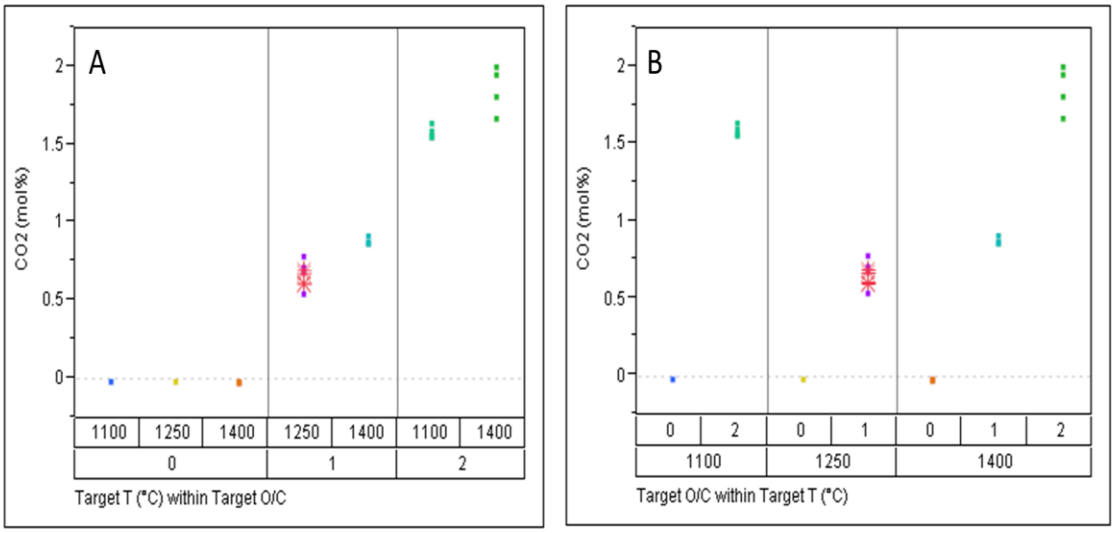

Figure 27: Variable statistics (A) CO_2 mole percent yield with respect to temperature within a given O/C ratio; (B) CO_2 mole percent yield with respect to O/C ratio within a given temperature.

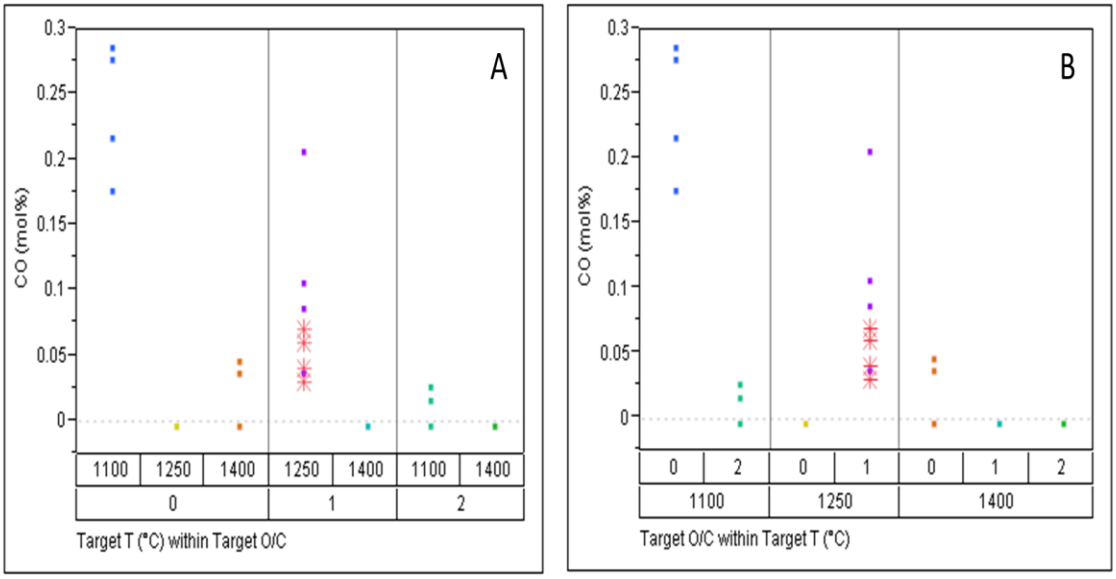

Figure 28: Variable statistics (A) CO mole percent yield with respect to temperature within a given O/C ratio; (B) CO mole percent yield with respect to O/C ratio within a given temperature.

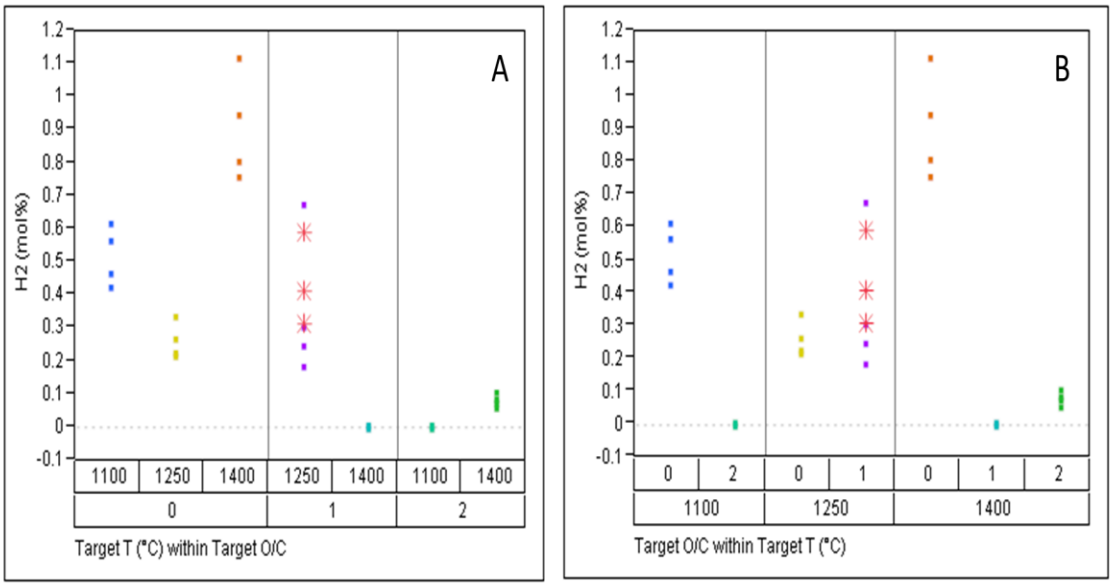

Figure 29: Variable statistics (A) H_2 mole percent yield with respect to temperature within a given O/C ratio; (B) H_2 mole percent yield with respect to O/C ratio within a given temperature.

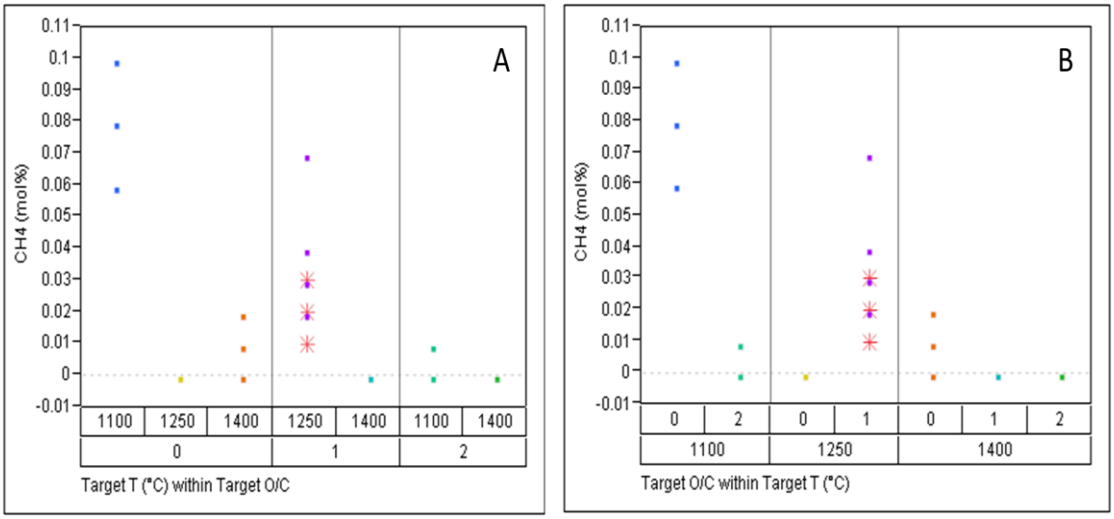

Figure 30: Variable statistics (A) CH_4 mole percent yield with respect to temperature within a given O/C ratio; (B) CH_4 mole percent yield with respect to O/C ratio within a given temperature.

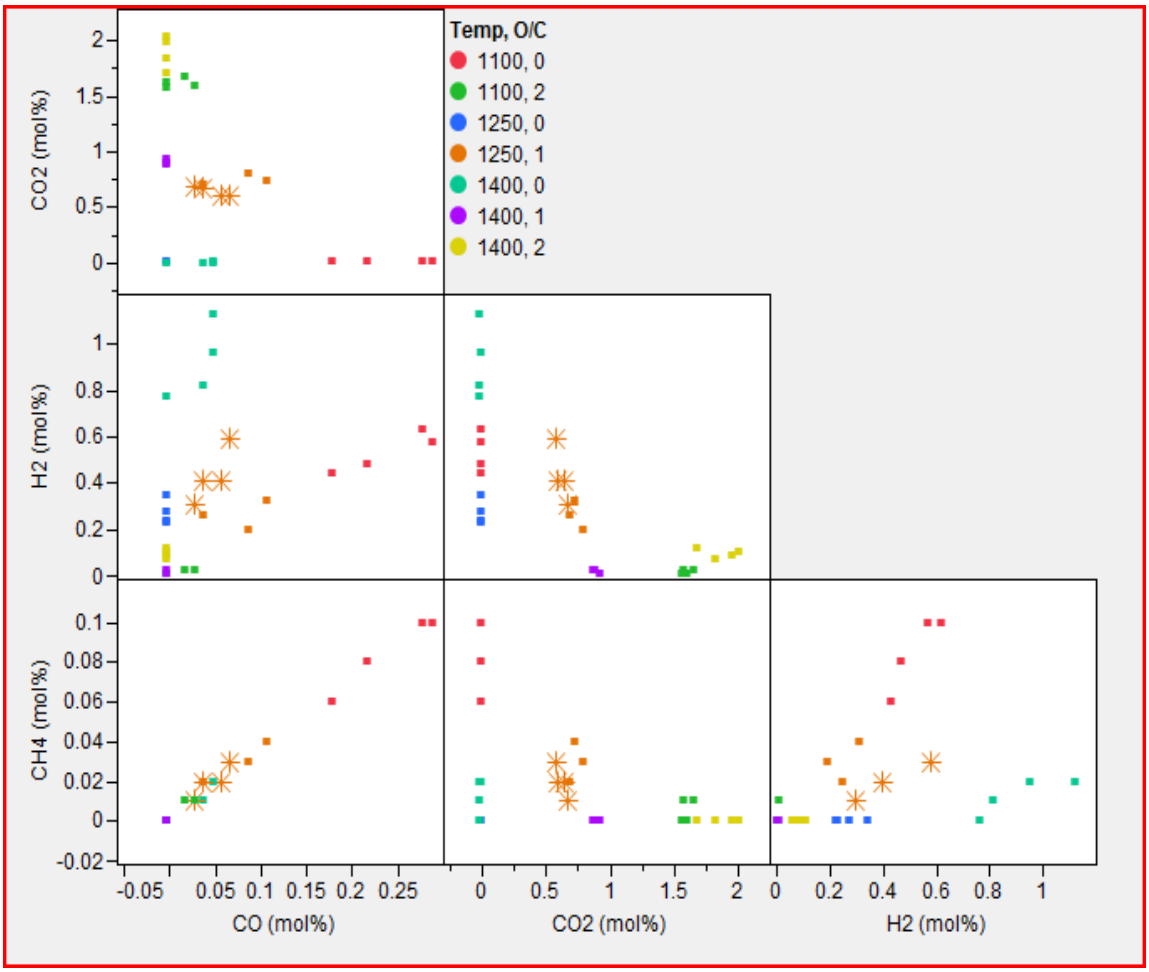

Figure 31: Major gas species data as a function of all other major gas species data

While Figure 31 appears more complex than the previous four figures, some important trends can be seen that indicate the relationships of CO_2, H_2, CH_4, and CO with one another. When plotting CH_4 and CO, a linear trend is seen signifying a strong relationship in which the concentration of one species heavily influences the other. For CH_4 and CO, when one concentration increases, the other increases proportionally. This is the opposite case when CO_2 and H_2 are plotted against each other where in the presence of zero CO_2, H_2 production increases with higher temperatures. A similar trend is present where near-zero concentrations of hydrogen indicate higher concentrations of

carbon dioxide at higher temperatures and even more with the combination of high oxygen content and high temperature. Qualitative trends beyond the few mentioned are difficult to note because the data points are ideally supposed to overlap, giving a tight distribution and minimizing deviation. This is not the case, however, and the above quantitative data for major gas species concentrations is incoherent to the level of neglecting the data on a practical basis. Since the data of the repeated runs were not reproduced and the deviation of most of the runs is high relative to the average, the gas phase data should be used only as a qualitative indicator of the laminar entrained-flow reactor's performance, not quantitatively. It is important to note that Figure 27 through Figure 31 only show data for Appalachian coal and no other solid fuel. This was the only fuel analyzed to this extent to offer a broad range of statistical data. Based on these results, the University of Utah and Eastman Chemical Company decided to use the gas-phase data qualitatively, not quantitatively.

4.1.3 Loss-on-Ignition Yields

Once the chars were produced, the 1400 ℃ samples were subjected to loss-on-ignition (LOI) testing. Table 16 displays LOI yields in which two LOI tests were conducted for each LEFR run; the range in average value is also given to express precision.

Figure 32 shows the data from Table 16, plotting the loss-on-ignition versus O/C ratio. By graphing the data, it is easier to note changes in LOI yield and to describe what is happening as oxygen is increased. The expectation is to observe decreasing char yield with increasing O/C and increasing temperature. From Figure 32, the data indicate an

Table 16: Loss-on-Ignition data for 1400 ℃ chars

Fuel	Run	LOI	LOI range	O/C Ratio
APP	2	86.60%	0.897%	2
APP	4	83.80%	1.335%	0
APP	8	71.12%	1.064%	1
EPC	2	98.84%	0.197%	2
EPC	4	94.89%	0.031%	0
EPC	8	92.03%	0.107%	1
TXL	2	17.61%	2.470%	2
TXL	4	50.53%	0.752%	0
TXL	8	24.62%	0.536%	1

inconsistency since the LOI yield first decreases for a middle oxygen content and then increase for both APP (A) and EPC (B). While Texas lignite data, plot (C), make the most sense of the three, the data lose creditability among the whole data set because plots (A) and (B) are so erratic. The following section proposes why the LOI and char yield data are so inconsistent and seemingly random in certain runs of the LEFR. The probable root cause stems from particle sizes of the chars.

Loss-on-ignition data and char yields disagree when statistically analyzed. In theory, the yields for both char and LOI should be the same because ash is used as a tracer and is assumed constant; inconsistencies are present in each data set as well. The generated trends, particularly for the Appalachian coal, show inconsistencies for both LOI and char yield data. After a discussion of experimental methods and reactor

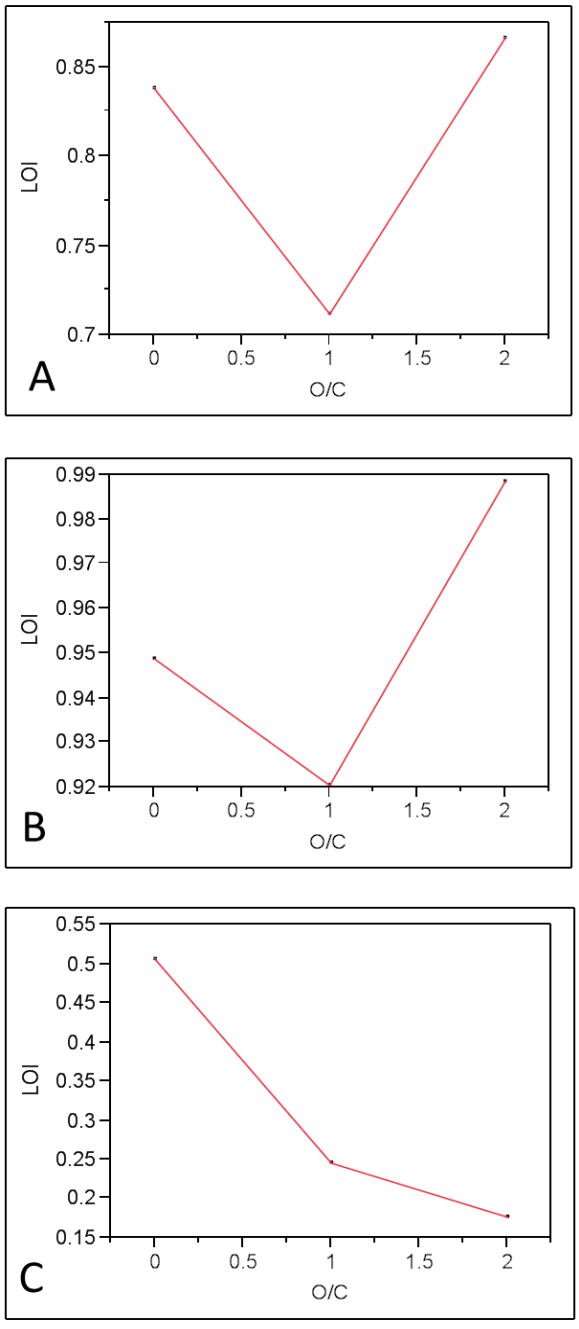

Figure 32: Bivariate analyses of LOI data for (A) Appalachian coal, (B) EPC petcoke, and (C) Texas lignite

robustness among Dr. Kevin Whitty, David Wagner, and Suhui Li, it was concluded that inconsistencies in LOI data most likely stem from the method used for the loss-on-ignition experiments conducted. The only noticeable difference in LOI methods carried out by David and Suhui was that Suhui sieved his char; a step that takes out most, if not all, agglomerated particles, but the calculations used to determine LOI data were identical. It is assumed the agglomeration of particles takes place as they exit the injection probe and are introduced to the reactor's high temperatures. Tar could evolve rapidly and act as a glue, holding particles together for the length of the reactor. If the agglomeration occurred in such a way, then carbon and volatiles would be 'trapped' within the adjoining particle interfaces, not allowing maximum potential conversion of the particle to occur. This theory was tested by sieving the char product from selected runs and performing LOI tests again. As per Suhui's experience and advice, the particles were sieved at roughly 150-200% of the initial average particle size of 400-200 mesh (38-74 microns); 150 mesh (104 micron) screen was used. The increase in mesh size accounted for particle swelling, but still kept out agglomerated particles. These LOI data are presented in Table 17 with corresponding O/C ratio, temperature, and particle size. 'Unsieved' particle sizes are the original data.

Three particle size ranges are given in Table 17 greater than 104 micron, less than 104 micron, and the original, unsieved char. For run 2 (O/C=2, 1400 ℃), the data show that more material is lost with larger or agglomerated particles, while there is a decrease in material lost for run 4 (O/C=1, 1400 ℃). These data suggest that final particle size and thus conversion of the fuel in the laminar-flow reactor influence loss-on-ignition values, and evidently much more than previously thought. The sieved runs in the table were only

Table 17: Sieved and unsieved (original) char particle results for LOI testing to determine cause of char run inconsistencies

Fuel	Run	Particle Size	% LOI	% Remaining	Test O/C	Temp °C
APP	2	>104 μm	86.992%	13.008%	2	1400
APP	2	Unsieved	87.234%	12.766%	2	1400
APP	2	Unsieved	85.965%	14.035%	2	1400
APP	2	<104 μm	65.789%	34.211%	2	1400
APP	4	>104 μm	79.747%	20.253%	0	1400
APP	4	Unsieved	84.746%	15.254%	0	1400
APP	4	Unsieved	82.857%	17.143%	0	1400
APP	4	<104 μm	84.615%	15.385%	0	1400

conducted once and were not repeated for the other solid fuels, EPC and TXL, because particle agglomeration was thought to be a factor in the production of APP chars largely based on the bituminous rank of the coal.

4.2 Pressurized Wire-Mesh Heater Studies

As prescribed in the Design of Experiments approach, triplicate testing was performed at the midpoint for all three fuels, a temperature of 1100 ℃, a pressure of 300 psig, and a hold time of 3.0 seconds. The average char yields of these runs are shown in Table 18 per fuel and include error at a 90% confidence level.

The error values from Table 18 can be applied to respective fuel types to quantify the error in each subsequent measurement without having to reproduce all conditions in triplicate (e.g. all error values for bituminous coal runs are assumed ±2.10% char yield).

Table 18: DoE triplicate runs for average char yields per fuel at a 90% confidence level.

Fuel	Average Char Yield	Error (90% CL)
Bituminous (APP)	69.0%	± 2.10%
Petcoke (EPC)	90.6%	± 1.43%
Lignite (TXL)	59.4%	± 4.29%

The trends found in other wire-mesh studies were also observed in this study. Char and volatile yields are tabulated in Table 19 along with corresponding run conditions. Yields that are starred (*) represent averages of more than one test under corresponding conditions; some runs were repeated under advisement of Eastman Chemical Company and some repeated based on the operator's experience. Due to a three-factor Design of Experiments, plotting the results becomes difficult. Two plots of the above data, one column plot and one radar plot, are found in Figure 33 and Figure 34, respectively. Comparing these two figures with each other and with Table 19, trends can be found and qualitative conclusions made.

While Figure 33 offers a traditional view of data, Figure 34 shows a quick qualitative perspective of the char yield data. For each lettered run condition, the values of the three fuels are compared against each other and trends are found. For example, beginning with condition A and moving clockwise, the char yield will increase, decrease, or remain relatively constant. Depending on the direction of change for the respective char yields, conclusions are made with respect to a specific factor found in Table 8. Figure 34 shows a rigid char yield trend concerning petcoke, which would certainly be attributable to a very low volatiles percentage and high percentage of fixed carbon. For

Table 19: Char and volatile yields of coal and petcoke wire-mesh heater runs with corresponding run conditions. Highlighted cells are averages.

Run	Run Conditions			Char Yield			Volatiles Yield		
	Final Temp (Celsius)	Pressure (psig)	Hold Time (seconds)	APP	EPC	TXL	APP	EPC	TXL
A	1000	0	1	81.1	94.1	59.9	18.9	5.9	40.1
B	1000	0	5	54.1	94.5	58.0	45.9	5.5	42.0
C	1000	900	1	68.2	96.6	87.7	31.8	3.4	12.3
D	1000	900	5	61.1	96.6	54.7	38.9	3.4	45.4
E	1100	300	3	69.0	90.6	59.4	31.0	9.4	40.6
F	1200	0	1	55.4	95.7	54.0	44.6	4.3	46.0
G	1200	0	5	52.6	90.0	51.0	47.4	10.0	49.0
H	1200	900	1	69.9	99.6	63.0	30.1	0.4	37.0
I	1200	900	5	67.1	89.9	91.8	32.9	10.1	8.3

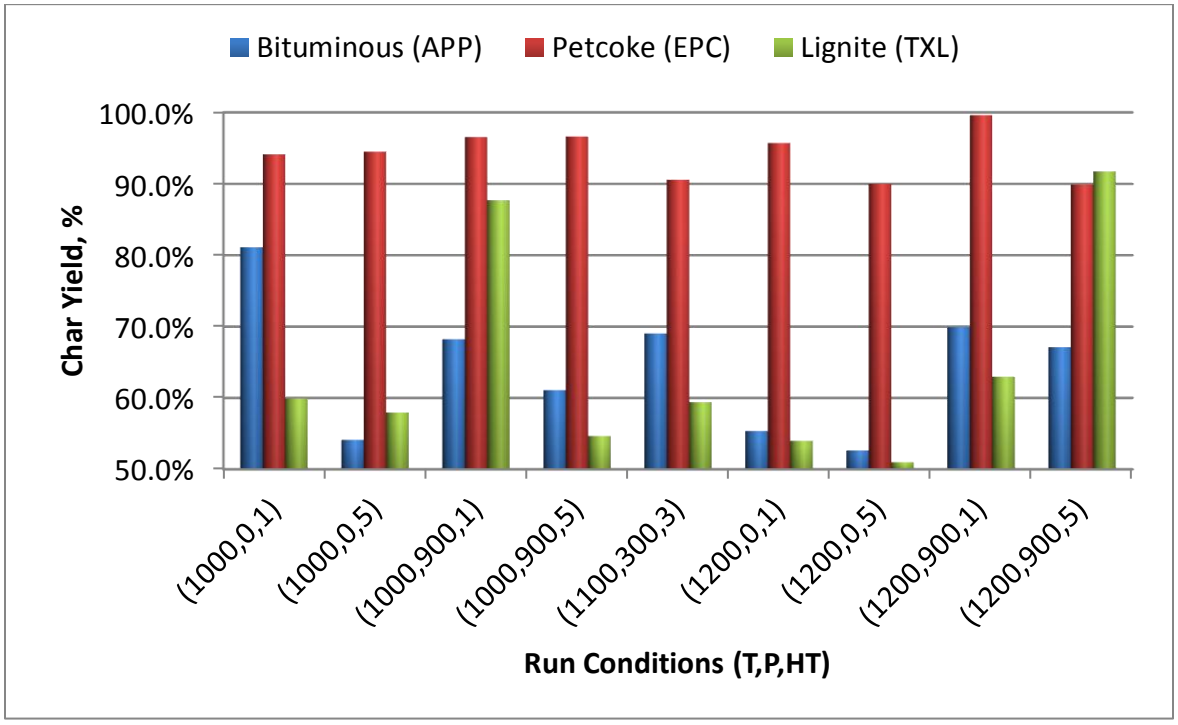

Figure 33: Char Yield (%) versus Run Conditions. The run conditions correspond to specified runs in Table 19

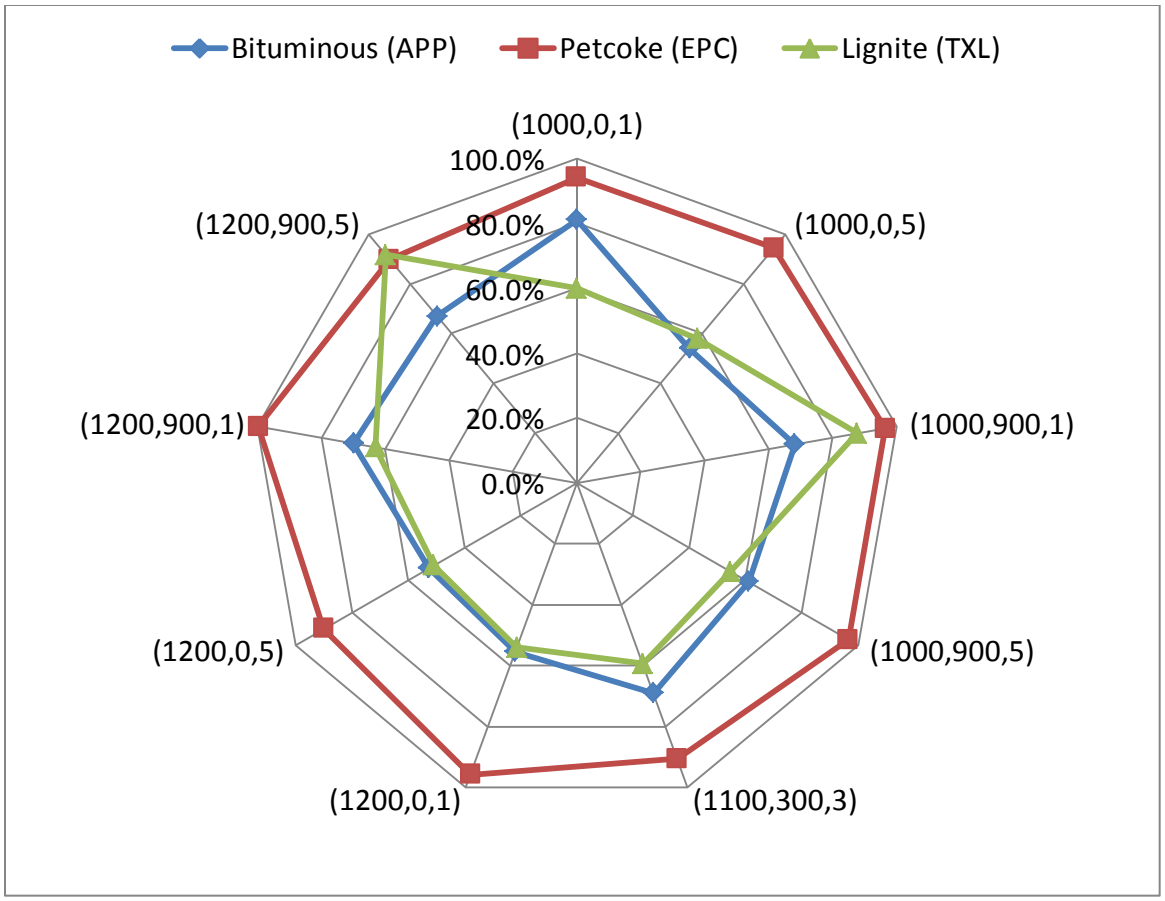

Figure 34: Radar plot of Char Yield (%) versus Run Conditions (T, P, HT).

the bituminous coal tests, as found in aforementioned studies, as pressure increases, the volatiles yield will decrease. This is exemplified in runs A and B versus C and D and runs F and G versus H and I, where A through D are at 1000 ℃ and F through I are at 1200 ℃. Here, runs C and I stand out to such a large degree that the char yields approach those of petcoke; since lignite has approximately four to five times more volatiles, this would be unexpected. Using variability charts, it becomes easier to compare data sets and find trends with respect to temperature, pressure, or hold time. Figure 35, Figure 36,

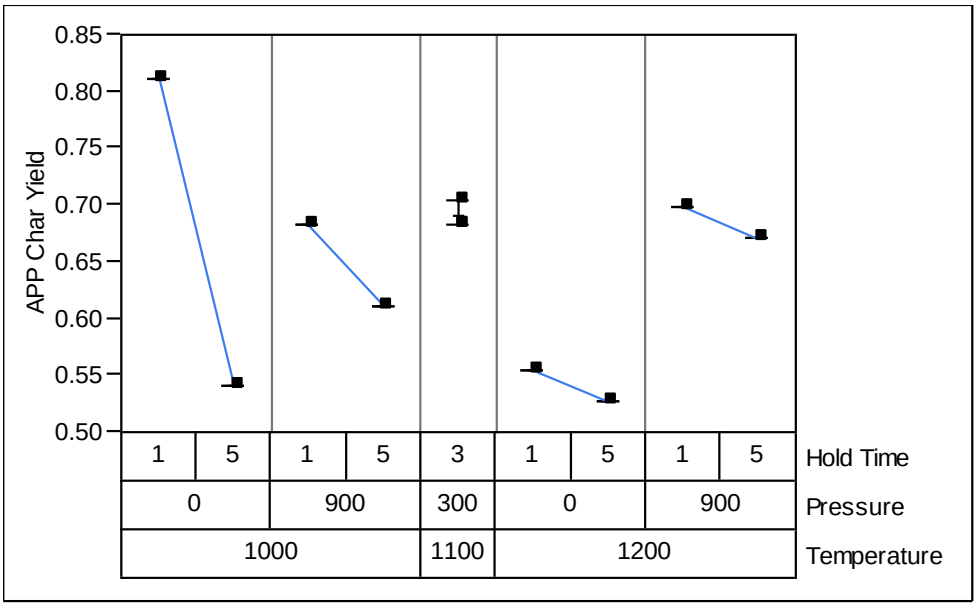

Figure 35: Variability chart: APP char yield versus run conditions.

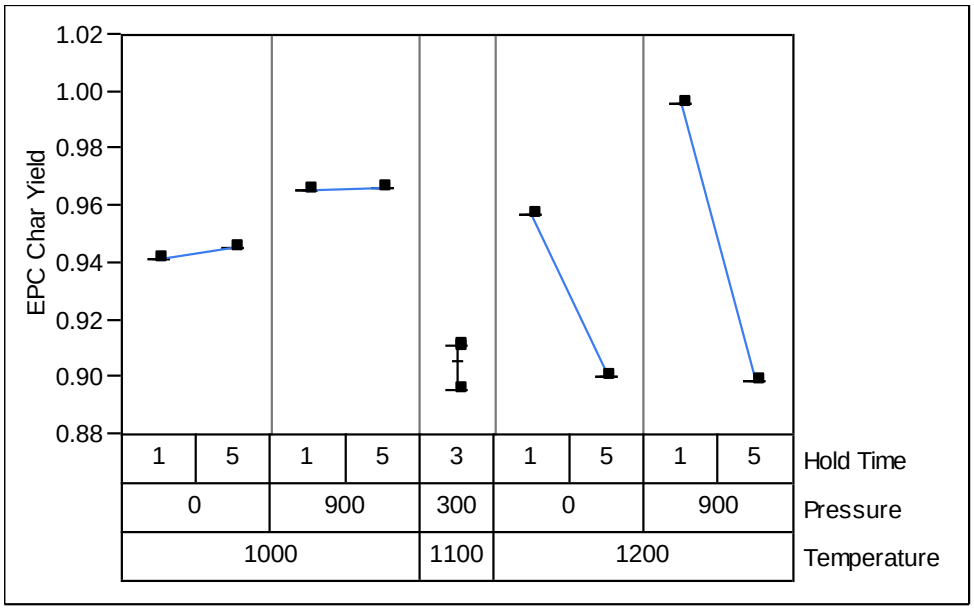

Figure 36: Variability chart: EPC char yield versus run conditions.

and Figure 37 show the char yields for bituminous (APP), petcoke (EPC), and lignite (TXL), respectively, versus the run conditions as per the Design of Experiments.

With the variability charts, it becomes easy to identify runs that appear unsuitable. Three points in particular stand out: APP at 1000 ℃, 0 psig, and 1.0 second hold time, TXL at 1000 ℃, 900 psig, and 1.0 second hold time, and TXL at 1200 ℃, 900 psig, and 5.0 seconds hold time. The operator noticed the APP run abnormality and ran two additional tests to verify the high char yield; the resulting mean of the three tests was 81.1% ±0.68% char yield (at 90% confidence level). Based on the repeated values of the APP case, the yields are plausible. The inconsistencies in the TXL fuel were not noticed until all testing was complete. Based on previous wire-mesh studies, it would not be wise to give credit to the two TXL char yield values and it is recommended that the tests be run again in triplicate to prove or disprove the results at hand. The error in yields for the two TXL cases is likely a result of operator error, but could also be from the fuel itself. The high volatile content of the lignite (27.8% as-received) coupled with the high water content (18.11% as-received) could cause the samples to devolatilize in a dissimilar manner via steam and volatile production depending on how the coal was applied to the mesh. Even though the fuels were applied to meshes by the same method, the physical geometry of particles and thickness of fuel on the mesh itself could be a source of error.

4.2.1 Wire-Mesh Heater Model Development

After successful completion of the wire-mesh heater test campaign, a model was created to predict future tests. A statistical program called JMP (version 7, SAS) was

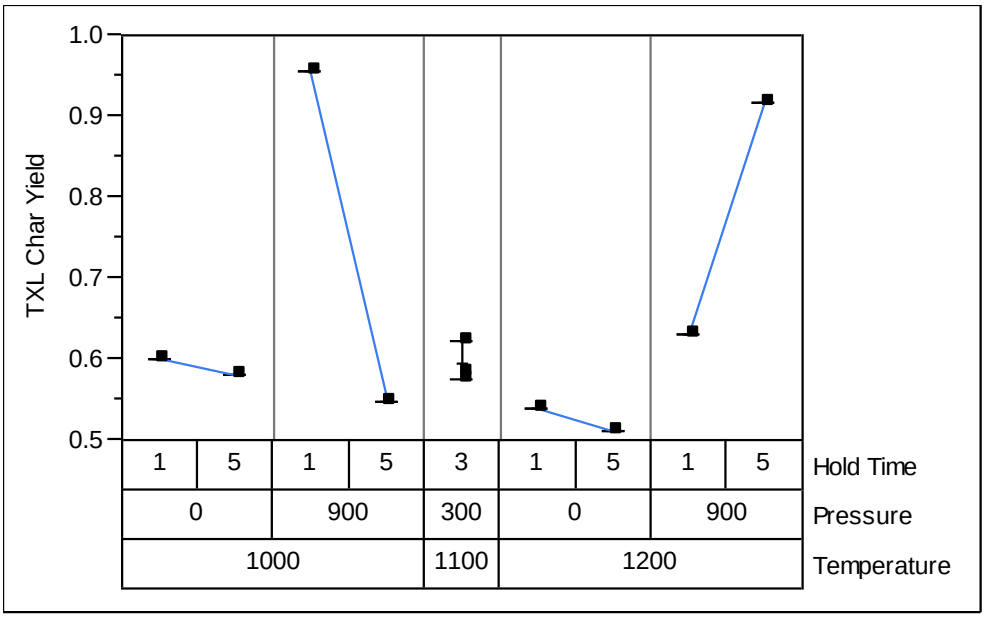

Figure 37: Variability chart: TXL char yield versus run conditions.

used to model the heater with respect to temperature, pressure, and hold time. The expression for the empirical model is below and corresponding constants are found in Table 20. Looking at the sign of each constant and the corresponding model per fuel, it is easy to discern the influence of the parameter on the char yield. All "A" constants are positive, indicating that there will be some char yield, no matter the conditions. This constant is a function of the average of the runs performed and is most likely dependent on the composition of the fuel much more so than the other parameters. Constants "B" and "C" act as a multiplier and average temperature over all runs, respectively. This indicates that as B decreases, char yield increases, as is expected. Also, as with pressure, P, as the constant "D" is increased, so is char yield. Hold time, as seen in constant "E", has a competing effect with pressure, in that as hold time is increased, char yield is decreased. Figure 38, Figure 39, and Figure 40 plot the char yield for temperature, pressure, and hold time influence, respectively. These plots were generated by taking the

Table 20: Empirical model constants for temperature, pressure, and hold time

	A	B	C	D	E
App. Coal	6.74E-01	-1.36E-04	1.07E+03	4.58E-04	-2.94E-02
Lignite	6.41E-01	-1.95E-05	1.12E+03	3.15E-03	-6.08E-03
Petcoke	9.38E-01	9.60E-05	1.08E+03	4.97E-04	-9.75E-03

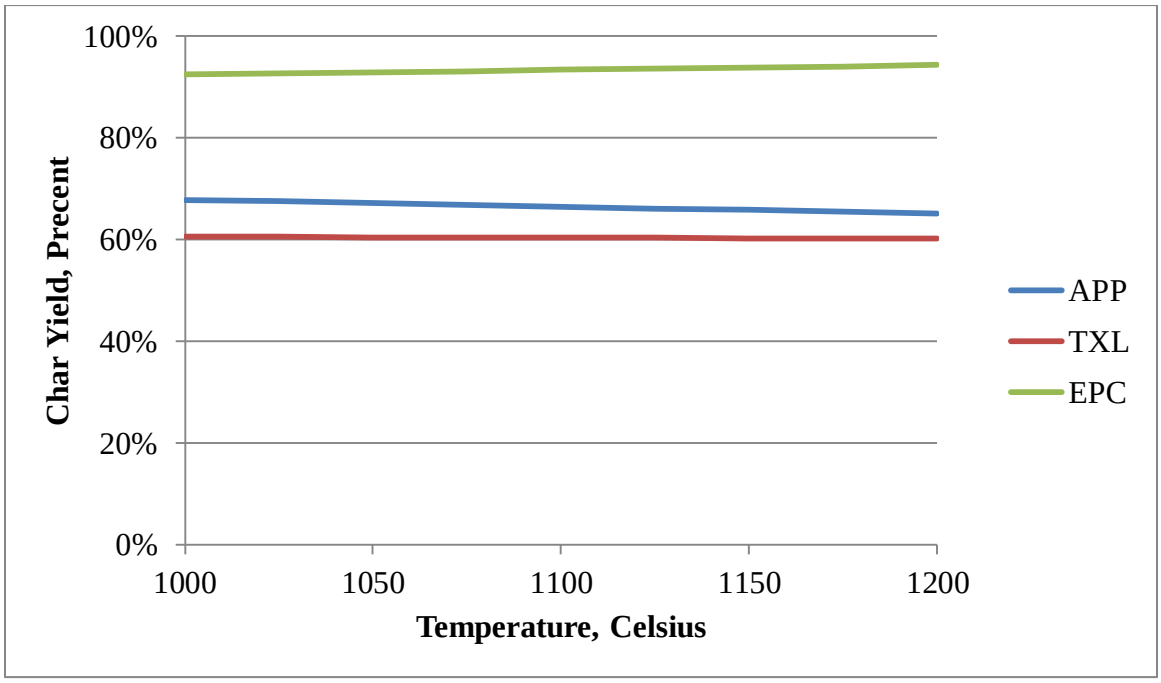

Figure 38: Empirical model verification: char yield versus temperature (at 20 bar and 3 second hold time)

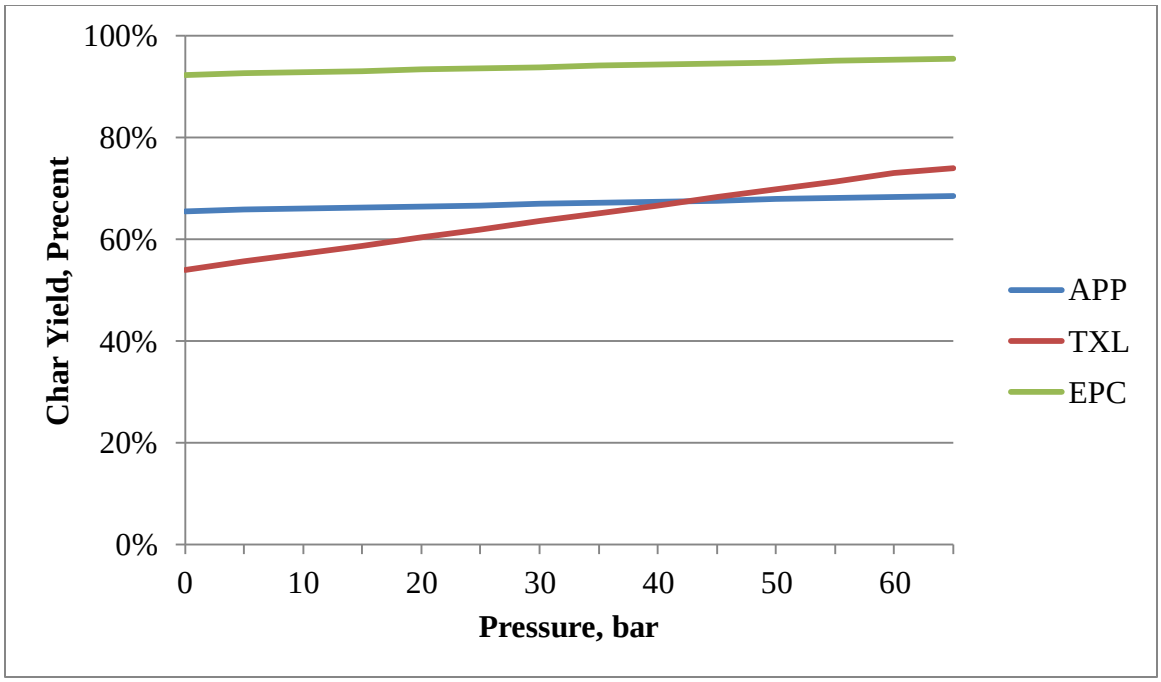

Figure 39: Empirical model verification: char yield versus pressure (at 1100 ℃ and 3 second hold time)

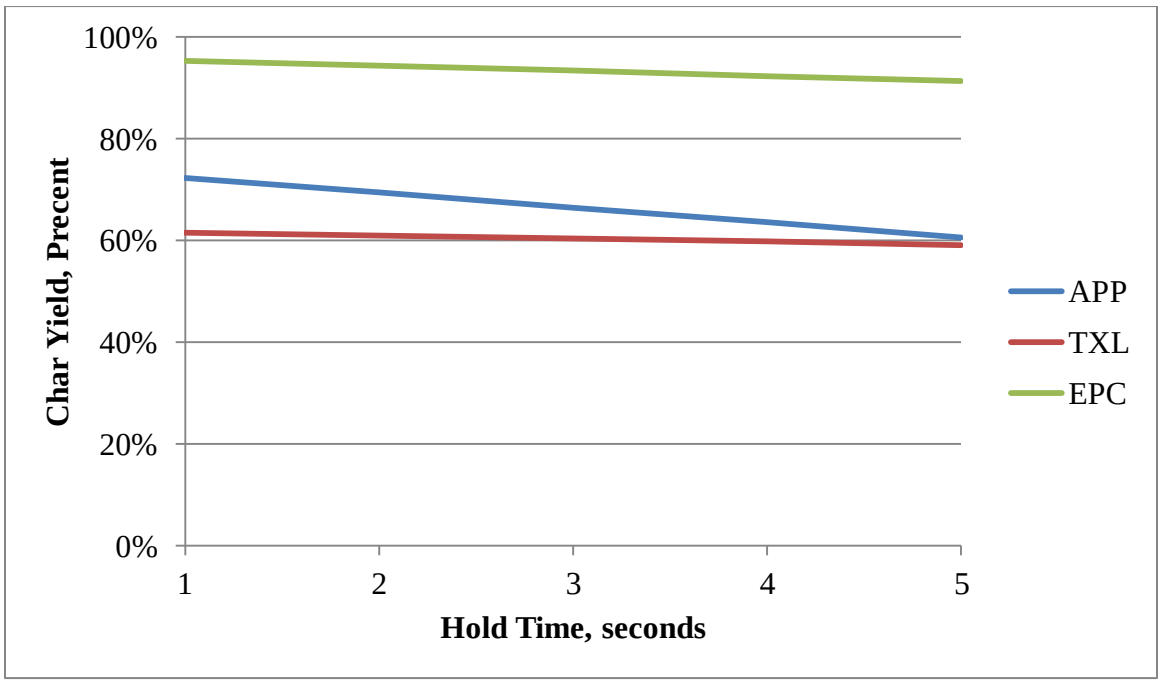

Figure 40: Empirical model verification: char yield versus hold time (at 1100 ℃ and 20 bar)

model parameters and filling a matrix of values between all tested values. Temperature ranges from 1000 ℃ to 1200 ℃, pressure from 0 psig to 900 psig (atmospheric pressure in Salt Lake City is 0.85 bar), and hold time from one to five seconds.

$$\text{Char Yield} = \text{A} + \text{B}\left(T - \text{C}\right) + \text{D}\left(P - 31.925\right) + \text{E}\left(H - 3\right)$$

These three model plots exhibit linear trends when holding the other values constant. It is possible that other factors will have an influence on char yield, such as quadratic effects and interdependent effects of the three factors (temperature, pressure, and hold time).

CHAPTER 5

CONCLUSIONS

5.1 Summary of Results

A great deal of information was learned during the experiments written about herein. The methods and data presented in this thesis are a verification of previous high temperature and high pressure studies both in pyrolysis and gasification as well as high pressure and moderate temperatures. While much of the data from the high temperature, atmospheric pressure tests left unanswered questions with respect to carbon conversion and gas species quantification, worthwhile efforts were made to verify the findings using previously proven methods like loss-on-ignition tests. Ultimately, the atmospheric pressure experiments are viewed as (a) the first time the laminar entrained-flow reactor was used to imitate an entrained-flow gasifier and (b) a failed experiment. Char, volatiles, and loss-on-ignition yields can be used as an indication of carbon conversion, while gas species data show to what extent temperature and oxygen have roles in that conversion.

The wire-mesh heater designed and fabricated at the University of Utah to study gasification behavior of coal and petroleum coke successfully reproduced trends in char and volatile yields that other studies have found. Pressure, final temperature, and holding time were varied to understand the influence of each factor on the gasification and

pyrolysis behavior of such fuels. While qualitative results suggest a correct method, quantitative results indicate how well the method accurately presents the data and if they agree with other wire-mesh studies.

The key contribution of this work stems from the use of petroleum coke. While the fuel itself has a high ratio of fixed carbon to volatile matter when compared to coal, industry still uses the fuel and with increasing energy demands, many businesses will be looking at how to use feedstocks that (a) already exist and (b) are less costly than newer technologies.

5.2 Implications for Pilot-scale Entrained-Flow Gasification

From a broad perspective, the data presented here can predict gasifier operation parameters and efficiencies if used appropriately. In commercial applications, however, such data would be verified repeatedly to reduce losses in profit and time before being implemented on large-scale gasification systems. Part of this verification can be performed in academia because it is less costly and the information obtained can be added to the whole body of knowledge. This facet of industry has been imperative for the work contained herein to have begun and progress, resulting in quality data and practical observations. Trends found in combining the high temperature, atmospheric pressure findings with those of the high pressure will be applied to the pilot-scale entrained-flow gasifier at the University of Utah's off-campus research facility to better understand the influence of pressure in conjunction with high temperatures. Oxygen content will become very important when operating with coal slurry injection and relatively high feed rates. Using the fundamental data found here, predictions are made

for the entrained-flow gasifier and then, in turn, that data will be scrutinized and most likely made available through journals or some other means to the Department of Energy and industrial partners.

5.3 Recommendations for Future Work

Based on all data and analyses presented herein, it is recommended that most results be used qualitatively and to learn from the quantitative problems encountered. The data that lack statistical confidence are urged to be repeated under conditions that are more rigid and leave less opportunity for error. While most of these statistically varied data are from the high temperature, atmospheric pressure tests, solutions to these problems are relatively easy and do not require a great deal more effort. In addition, it is recommended that specific tests from the wire-mesh campaign be run again to validate the current wire-mesh heater operating method and verify the Texas lignite (TXL) and Appalachian coal (APP) char yields that appear to be incorrect. These tests will be re-run at the behest of Eastman Chemical Company.

Future testing is recommended to offer a wider range of final temperatures and offer a more complete Design of Experiments to fill in the gaps of the data presented herein. Larger sample sizes for wire-mesh tests are proposed to measure elemental compositions of the chars and quantify the influence of factors affecting gasification behavior to aid in industrial processes.

APPENDIX

WIRE-MESH HEATER STANDARD

OPERATING PROCEDURE

1. Weld R-type thermocouple leads to the grid in the middle of the folded mesh. The mesh should be 2.5 inches by 1.0 inch.
2. Ensure the solid-state contactor/relay (SSR) is in the OFF position as well as the DC power source. Place the mesh and thermocouple in the pressure vessel and connect the thermocouple blocks. Insert the mesh between the copper block extensions and tighten the setscrew.
3. Make sure the LabVIEW software is reading a valid temperature and that the thermocouple leads are not touching the mesh at multiple points or each other.
4. Place the top flange on the pressure vessel with a Garlock 3000 gasket and bolt it down.
    a. If pressurizing the vessel above atmospheric, use a minimum torque specification of 131 ft-lbs. For tests at 300 and 900 psig, use the preferred torque specification of 200 ft-lbs.
    b. When achieving a pressure of 0 psig, 80 ft-lbs of torque will suffice.
5. Connect the tubing to the top flange that leads to the pressure gauge and relief valve.

6. Close the secondary valve on the regulator of the gas cylinder, then open the cylinder.
7. Open the relief valve and slowly open the secondary valve on the regulator, allowing gas to run through the system. When purging the system, 80 liters of gas (nitrogen) is enough to remove all detectable levels of oxygen. This was verified using a Varian CP-4900 microgas chromatograph.
8. When 80 liters of gas has run through the system according to the dry-gas meter (DGM), close the secondary regulator valve first, then the relief valve.
    a. If running a 0 psig test, the pressure vessel is ready for PID characterization.
    b. If running a 300 or 900 psig test, open the secondary regulator valve while keeping the relief closed. Open the regulator valve as necessary to achieve the desired pressure.
9. Since each mesh/thermocouple pairing is slightly different, the power output must be set each time. Within the LabVIEW Front Panel display under the Control Settings group, change the 'upper limit' output to achieve the desired ramp and soak profile and final temperature; the PID gain schedule should be set already, but can be altered if necessary. Turn on the SSR and DC power supply and run the setpoint profile until the desired values are reached.
10. After the power output and PID gains are set for the test, turn off the DC power supply and SSR and slowly open the relief valve to release any pressure and wait until the pressure inside the vessel is at atmospheric.

11. Once atmospheric pressure is achieved in the vessel, remove the top flange and gasket. Wearing disposable gloves, so as not to contaminate the mesh or thermocouple, place the mesh in a weigh boat. Record the weight of the individual boat first, then the mesh/thermocouple assembly with the boat.
12. Open the folded mesh and add approximately 20 to 30 milligrams of fuel. Record the new total weight (fuel + mesh/thermocouple assembly + boat). The fuel should be sieved before to a size above 500 Tyler mesh to not fall through the mesh.
13. Reconnect the thermocouple blocks and gently place the mesh between the copper block extensions. Make sure no fuel falls off and that the thermocouple wires are not touching the mesh in multiple locations.
14. Open the LabVIEW interface to ensure the thermocouple is still reading an accurate value.
15. Place the top flange back on the pressure vessel with a new gasket; do not reuse the same one if pressurizing above 0 psig. Connect the exit tubing to the top of the flange.
16. Close the secondary regulator valve and open the relief valve. Open the cylinder and slowly open the secondary valve. Allow at least 80 liters of nitrogen (or gas) to purge the system of any oxygen.
17. After purging, close the secondary regulator valve and allow the pressure inside the vessel to come to atmospheric; then close the relief valve.
    a. If conducting a 0 psig test, leave both the secondary regulator valve and the relief valve closed.

b. If conducting a 300 or 900 psig test, slowly open the secondary regulator valve and allow the vessel to come up to pressure. Do not use the pressure gauge on the regulator as an indication of the pressure inside the vessel; use the pressure gauge on the outlet near the relief valve.

18. When the pressure vessel reaches the desired pressure, close the valve on the gas cylinder. This is a safety precaution in the event the vessel looses pressure.
19. Turn on the DC power supply and SSR.
20. Using the LabVIEW interface, double-check the temperature reading and Control Settings. In the 'save data' box under file name, change the '.tdms' file following the convention, Date-Fuel-Final Temperature-Pressure-Hold Time-Run No. (e.g. 100812-APP-1100-900-3-22; the date is year/month/day; the fuel types are APP (Appalachian bituminous), TXL (Texas lignite), and EPC (Eastman petcoke); the final temperature is either 1000, 1100, or 1200 (Celsius); the pressure is either 0, 300, or 900 (psig); the hold time is either 1, 3, or 5 (seconds); the run number signifies the order in which all tests are carried; it will range from 1 to 33).
21. Double check all PID settings and gain scheduling values. Make sure the 'upper limit' in the Control Settings portion of the Front Panel Display is set at the desired value and that the setpoint profile is properly adjusted for a heating rate of 1000 ℃/s and the hold time and final temperature are adjusted for the specific run.
22. When all values and pressures are at desired values, click the 'Start Profile' button next to the plot on the right-hand side of the screen and allow the profile to run until completion.
23. When the run is finished, turn off the DC power supply and SSR.

24. Make sure the gas cylinder valve is closed, and slightly open the relief valve to depressurize the vessel.
25. Once the checker on the DGM is no longer moving, begin loosening the bolts on the pressure vessel flanges. Do this carefully so as not to shake the vessel and cause fuel to fall from the mesh.
26. After removing the top flange, tare a weighing boat and carefully unscrew the Allen screws at the top of the copper blocks. Place the mesh apparatus with thermocouple connector block in the boat and weigh. Record the value.
27. Char yield is calculated as 'weight of fuel after' divided by 'weight of fuel before.' Volatiles yield is 100% minus the char yield.

REFERENCES

1. Lowry, H. H., *Chemistry of Coal Utilization*; Wiley and Sons: New York, 1981; Vol. Second Supplementary.

2. Solomon, P. R.; Colket, M. B., Coal Devolatilization. In *Symposium on Combustion*, 1984.

3. Shadle, L.; Berry, D., Coal Gasification. In *Kirk-Othmer Encyclopedia of Chemical Technology*; Wiley and Sons: New York, 2009; Vol. 6.

4. Anthony, D.; Howard, J.; Hottel, H.; Meissner, H., Rapid Devolatilization and Hydrogasification of Bituminous Coal. *Fuel* **1976,** *55*, 121-128.

5. Harris, D. J.; Roberts, D. G.; Henderson, D. G., Gasification Behaviour of Australian Coals at High Temperature and Pressure. *Fuel* **2006,** *85*, 134-142.

6. Merrick, D., *Coal Combustion and Conversion Technology*; Elsevier Science Ltd: New York, 1984.

7. Qadar, S. A., *Coal Science and Technology 8: Natural Gas Substitutes from Coal and Oil*; Elsevier Science Ltd: New York, 1985.

8. Rezaiyan, J., *Gasification Technologies*.; CRC Press: Boca Raton, FL, 2005.

9. Wen, C. Y., *Entrained-bed Coal Gasification Modelling*; Industrial and Engineering Chemistry Process Design and Development, 1979.

10. Zeng, D.; Clark, M.; Gunderson, T.; Hecker, W.; Fletcher, T., Swelling Properties and Intrinsic Reactivities of Coal Chars Produced at Elevated Pressures and High Heating Rates. *Proceedings of the Combustion Institute* **2005,** *30*, 2213-2221.

11. Gibbins, J. R.; King, R. A. V.; Wood, R. J.; Kandiyoti, R., Variable-heating-rate Wire-mesh Pyrolysis Apparatus. *Review of Scientific Instruments* **1989,** *60* (6), 1129-1139.

12. Suuberg, E. M.; Peters, W., A.; Howard, J. B., A Comparison of the Rapid Pyrolysis of a Lignite and Bituminous Coal. *Thermal Hydrocarbon Chemistry* **1979**, *183*, 239-257.

13. Sathe, C.; Hayashi, J.-I.; Li, C.-Z., Release of Volatiles from the Pyrolysis of a Victorian Lignite at Elevated Pressures. *Fuel* **2002,** *81* (9), 1171-1178.

14. Stojiljkovic, D.; Radovanovic, M.; Ercegovac, M.; Jones, J. M.; Williams, A., Devolatilization of Some Pulverized Eastern European Lignites. *Journal of the Energy Institute* **2005,** *78* (4), 190-195.

15. Higman, C.; van der Burgt, M., *Gasification*; Elsevier Science Ltd: New York, 2003.

16. Schilling, H.-D.; Bonn, B.; Krauss, U., *Coal Gasification: Existing Processes and New Developments*; Graham & Trotman: London, 1979.

17. Crewe, G.; Gat, U.; Dhir, V. K., Decaking of Bituminous Coals by Alkaline Solutions. *Fuel* **1975,** *54*, 20-23.

18. Serio, M. A.; Solomon, P. R.; Heninger, S. G., Coal pyrolysis in a high pressure entrained flow reactor. *Preprints of Papers - American Chemical Society, Division of Fuel Chemistry* **1986,** *31* (3), 210-221.

19. Lowry, H. H., *Chemistry of Coal Utilization*. John Wiley: New York, 1945; Vol. 1.